NATIONAL AERONAUTICS AND SPACE ADMINISTRATION

Technical Report No. 32-532

Kinetics of Graphitization

I. The High-Temperature Structural Transformation in Pyrolytic Carbons

D. B. Fischbach

N66-16152

FACILITY FORM 602

(ACCESSION NUMBER) 46	(THRU) 1
(PAGES) CR 69917	(CODE) 18
(NASA CR OR TMX OR AD NUMBER)	(CATEGORY)

GPO PRICE $ _____

CFSTI PRICE(S) $ _____

Hard copy (HC) 2.00

Microfiche (MF) .50

ff 653 July 65

JET PROPULSION LABORATORY
CALIFORNIA INSTITUTE OF TECHNOLOGY
PASADENA, CALIFORNIA

February 1, 1966

NATIONAL AERONAUTICS AND SPACE ADMINISTRATION

Technical Report No. 32-532

Kinetics of Graphitization I. The High-Temperature Structural Transformation in Pyrolytic Carbons

D. B. Fischbach

C. E. Levoe, Manager
Materials Section

JET PROPULSION LABORATORY
CALIFORNIA INSTITUTE OF TECHNOLOGY
PASADENA, CALIFORNIA

February 1, 1966

Copyright © 1966
Jet Propulsion Laboratory
California Institute of Technology

Prepared Under Contract No. NAS 7-100
National Aeronautics & Space Administration

CONTENTS

TABLES

FIGURES

ABSTRACT

Under heat treatment at high temperatures, pyrolytic carbons (pyrolytic graphites) undergo an extensive structural transformation (graphitization). Layer stacking order, crystallite size, and preferred orientation increase. There are associated changes in macroscopic dimensions and optical microstructure. The kinetics of this graphitization transformation has been investigated for several pyrolytic carbons in the temperature range 2400–3000°C. The transformation was found to be thermally activated, with an effective activation energy of about 260 kcal/mole. The fundamental graphitization process appeared to be the same for all of the carbons studied, but there were differences in their detailed kinetic behavior associated with differences in as-deposited microstructure. Substrate nucleated carbons deposited under the usual conditions graphitized in a succession of stages of first-order form. In regeneratively nucleated and low-deposition-temperature carbons these stages were broadened and could not always be resolved. Variations in both the rate and the mode of transformation can be understood in terms of the dependence of the graphitization process on apparent crystallite layer diameter. A simple model of the graphitization process consistent with these observations is discussed. The significance of these observations for engineering applications is considered briefly.

I. INTRODUCTION

Graphite is the stable crystalline form of carbon at ordinary ambient pressure. It has a hexagonal crystal structure with an ordered ABABAB basal-plane stacking sequence.* The unit-cell height c (twice the interlayer spacing) is 6.708 Å; the unit-cell width a (basal-plane lattice parameter) is 2.462 Å. Pregraphitic synthetic carbons have a similar structure, except that the stacking sequence is randomly disordered (turbostratic structure). For a completely turbostratic carbon, $c \geqq 6.88$ Å. When turbostratic carbons are heated to high temperatures, graphitization tends to occur, the layer stacking evolving toward the ordered sequence of graphite with a consequent decrease in c. The fractional change in unit-cell

*There is an alternate ordered structure for graphite, the rhombohedral form, characterized by an ABCABC stacking sequence. Up to about 30% rhombohedral form can be produced from hexagonal graphite by appropriate mechanical treatment. However, it is metastable and reverts to the hexagonal form on heating to temperatures above 1000°C (Ref. 1).

height, $g = (6.88 - c)/0.172$, is a convenient measure of the degree of graphitization. Crystallite growth also occurs, and in many cases an increase in preferred orientation is observed in the graphitizing particles. This graphitization transformation takes place much more readily in certain types of carbon (pyrolytic, petroleum or pitch coke, etc.) than in others (glassy carbons, carbon blacks, etc).

The process by which graphitization occurs is complex and is not well understood despite its fundamental importance to the science and technology of carbon and graphite. Information on the kinetics of the process should be helpful in determining the detailed mechanism. However, until recently there has been a notable lack of information on this subject. In fact, it has been the general belief that graphitization is relatively insensitive to heat-treatment time and depends primarily on maximum heat-treatment temperature. Thus it has been common practice to specify the structure of a soft (graphitizing) carbon in terms of maximum treatment temperature, often with little concern for treatment time or conditions. During the last few years there has been increasing evidence that this viewpoint is inadequate. Numerous studies (Refs. 2–12) on conventional soft carbons (petroleum coke, coal-tar pitch coke, etc.) have shown that there is a strong dependence of degree of graphitization on heat-treatment time as well as on treatment temperature and have indicated that graphitization is probably a thermally activated process. However, the structures of these carbons are complex and poorly defined, and the kinetic behavior is difficult to interpret.

Within the last few years, a different type of synthetic pregraphitic carbon has become available. This is pyrolytic carbon (commonly misnamed pyrolytic graphite). It is formed by the thermal decomposition of a hydrocarbon gas (usually methane) and deposition of the carbon on a hot substrate (usually conventional synthetic graphite) at temperatures in the range 1800–2300°C. Such deposits are quite pure and have near-theoretical densities. The structure consists of turbostratic crystallites of 150–350 Å apparent diameter and 100–250 Å apparent thickness, with the basal planes oriented approximately parallel to the substrate surface. The microstructure exhibits characteristic "growth cone" features and may conveniently be approximated by a model consisting of a stack of wrinkled sheets. When pyrolytic carbons are heat-treated at temperatures above the deposition temperature, they undergo an extensive structural transformation somewhat reminiscent of recrystallization in cold-worked metals. Layer ordering occurs, crystallite size and preferred orientation increase, and the cone microstructure coarsens and may ultimately disappear. As a consequence of these structural changes, there are also changes in macroscopic dimensions.

Because of its unique structure (large crystallite size combined with random layer stacking), high purity, density, and preferred orientation, pyrolytic carbon is a much better research material for studying fundamental processes in carbons than conventional synthetic (or natural) carbons. Relatively little attention has been given to the kinetic aspects of the transformation in pyrolytic carbons. It has been variously reported that there is a saturation partial degree of graphitization which increases with heat-treatment temperature (Ref. 13), that there is a well-defined graphitization temperature (Ref. 14), and that above 2600°C the degree of graphitization increases with isothermal annealing time without an incubation period (Ref. 15). Therefore, it appeared worthwhile to investigate the high-temperature transformation in these materials in some detail in the hope that increased understanding of the kinetics and mechanism of the graphitization process might be gained. In addition, because of the attendant property changes, the transformation may have important consequences for the practical application of pyrolytic carbons at high temperatures.

The present report is concerned exclusively with the kinetic aspects of the graphitization and associated structural changes in pyrolytic carbons heat-treated in an inert gas atmosphere under zero applied stress. Possible effects of reactive atmospheres, catalysts, and stress or plastic deformation on the transformation are not considered here. Some preliminary results of this investigation have been published elsewhere (Refs. 16–18). A later report, Part II of this series, will deal with the kinetics of graphitization in conventional synthetic carbons (petroleum coke, coal-tar pitch coke, and composites of these two).

II. EXPERIMENTAL PROCEDURE

The general procedure followed in this investigation was to observe changes in the structure and properties of pyrolytic carbons as a function of isothermal heat-treatment time at various treatment temperatures. All such measurements were made at room temperature. Parameters measured included unit-cell height, preferred orientation, apparent crystallite diameter, and diamagnetic susceptibility. Microstructure changes were also observed.

A. Materials

Seven different pyrolytic carbons, obtained from two commercial producers, were investigated. They were deposited from methane under essentially isothermal conditions at temperatures ranging from 1800 to 2200°C. Information on these carbons is summarized in Table 1. A variety of as-deposited microstructures was represented as shown in Fig. 1. These micrographs were obtained with polarized light and the contrast results from variations in basal-plane orientation. The structures of carbons A through D are similar and are typical of the structures usually encountered in pyrolytic deposits of this type. Nucleation of the growth cones occurs primarily on the substrate surface, though some additional nucleation occurs throughout the deposit. Carbon G has an unusually coarse substrate nucleated structure, while the structure of E appears to be intermediate between that of A–D and F. Carbon F represents the regeneratively (or continuously) nucleated type of structure which results from deposition under conditions which promote the formation of soot particles in the gas phase and inclusion of these particles in the deposit.

Although no chemical analyses were performed on these materials, all are believed to be of high purity. Carbon A was deposited in a special "clean" run using chemically pure (C.P.) (99.4%) methane, and carbon C was also reported to have been made from C.P. gas. The remainder of the sample materials were deposited from commercially pure methane or natural gas. Horton (Ref. 19) has reported the results of analysis of a lot of pyrolytic carbon deposited from natural (city) gas. He found metallic impurities to be below the limit of sensitivity of the spectroscopic technique used, while a 15-min heat treatment at 1000°C in vacuum released quantities of CO_2, CO, H_2, CH_4, and H_2O ranging from 0.002 wt% CO to 8×10^{-6} wt% H_2O. Additional measurements on similar material by Smith (Ref. 20) indicated the existence of 0.005 wt% ash consisting principally of Fe, Si, and Mg, probably picked up from the conventional synthetic graphite substrate, and showed that less than 5 ppm of hydrogen were released by heating a powdered sample for long times at 2000°C in vacuum. Quantities of other gases released during outgassing at 500°C in vacuum in the latter measurement were attributed to adsorption in the powdered sample.

Table 1. Some deposition and structural parameters of the carbons investigated

Carbon	Deposition temperature* °C	Source gas*	Microstructure	Unit-cell height c, Å	Apparent crystallite diameter L_a,† Å	Preferred-orientation parameter n	Bulk density, g/cm³	Producer
A	2150	C.P. methane	Medium-fine primary	6.85	220–260	8	2.18	High Temperature Materials, Inc.
B	2100	C.P. methane	Medium-fine primary	6.85	320–350	8	2.21	High Temperature Materials, Inc.
C	1900	Methane	Medium-fine primary	6.85	240–310	10	2.21	High Temperature Materials, Inc.
D	2200	Natural gas (methane)	Medium-fine primary	6.84	260–310	8	2.20	General Electric Co.
E	2200	Natural gas (methane)	Medium-fine primary	6.85	250–320	8	2.20	General Electric Co.
F	2100	Natural gas (methane)	Regenerative	6.86	≈240	6	2.16	General Electric Co.
G	1800	Natural gas (methane)	Coarse primary	6.84	≈150	10	2.06	General Electric Co.

* Information supplied by producer.
† Estimated from magnetic susceptibility.

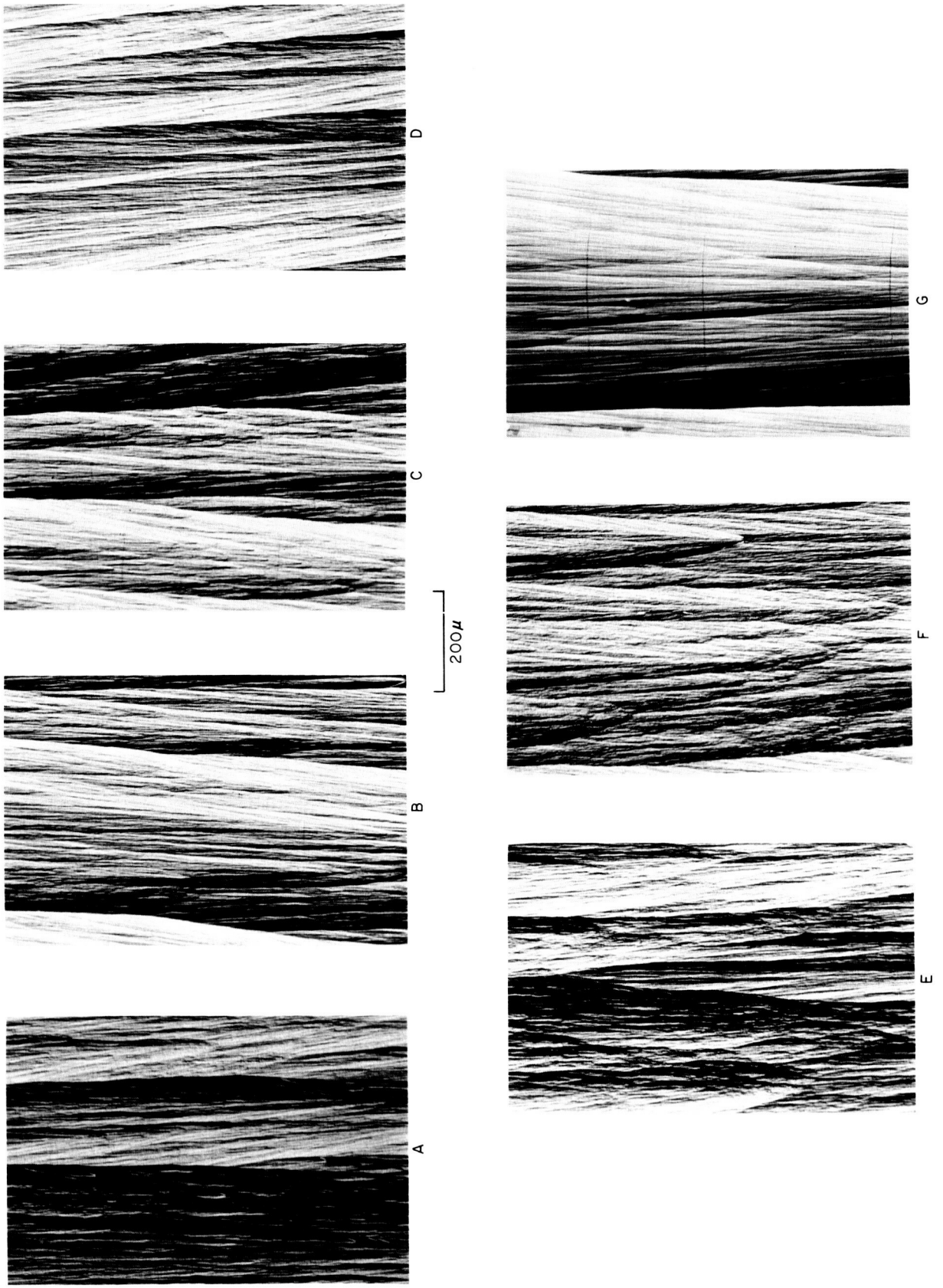

Fig. 1. As-deposited microstructures of the carbons studied; the substrate side of the deposit is toward the bottom of the photographs

B. Measurement Techniques

The progress of the transformation was followed by both x-ray diffraction and magnetic-susceptibility measurements at room temperature as a function of isothermal heat-treatment time. The unit-cell height c was determined from the position of the (004) diffraction peak using the Debye–Scherrer technique with Ni-filtered Cu Kα radiation and a 114.6-mm-diam camera with the Straumanis film arrangement. Peak positions were determined visually using a standard film reader. Ideally, lattice parameters should be determined from the positions of strong, sharp peaks at high Bragg angles to reduce systematic errors and possible absorption effects. The (00l) layer-plane diffraction peaks with $l = 2$, 4, 6, and 8 (Bragg angles of approximately 13, 27, 43, and 65 deg, respectively) are produced by the Cu characteristic radiation. The (002) is very strong, but it occurs at a low angle and its position is difficult to measure accurately because of its width and strong curvature on the film. The highest angle peaks are not satisfactory either. The (006) is very weak and tends to overlap the (112) peak in the early stages of graphitization. The (008) is too weak and broad to measure until an appreciable amount of graphitization has occurred. Therefore, the (004) peak was used because it was the highest angle peak which could be measured with some precision over the whole graphitization range.* The precision of the unit-cell height measurement was estimated to be $\pm 0.1\%$ or better. The proportion of correctly ordered layers has been related to the unit-cell height in a number of ways, but it is not clear which of these expressions is the most realistic. Therefore, the unit-cell height itself was used as the measure of the progress of the graphitization transformation in the present work.

An approximate value of the apparent crystallite layer diameter L_a was calculated from the position of the (10) or (100) diffraction peak by Warren's formula for turbostratic carbon (Ref. 21),

$$L_a = [a/(a - a')]\,(0.16\,\lambda/\sin\theta)$$

where $a = 2.4615$ Å (the graphite value), a' is the apparent a value determined from the position of the maximum intensity of an (hk) diffraction band, λ is the x-ray wavelength, and θ is the Bragg angle of the diffraction maximum. This technique can be applied directly to visual reading of Debye–Scherrer films. A simple error analysis shows that the probable error increases quite rapidly with L_a for values above about 100 Å, but with care useful approximate values can be determined in the higher range. It may be questioned whether this technique is valid after the two-dimensional (10) peak begins to modulate into the three-dimensional (100), (101), etc. with the development of layer order. However, Bacon and Franklin (Ref. 22) reported a definite shift in ($hk0$) peak positions attributed to crystallite size effects even in fairly well graphitized carbons. Further evidence that this technique works for partially graphitized pyrolytic carbons will be presented in Sec. III. It is believed that the L_a values determined here are at least qualitatively significant for L_a less than about 500 Å. For larger diameters, the precision of the present x-ray measurements does not justify much confidence in the results.

In general, the Debye–Scherrer patterns were obtained from powdered samples. A quantity of powder was prepared by filing the as-received carbon and sieving through a 325-mesh screen prior to heat treatment. A small portion of the powder was removed after each treatment and a glass capillary (0.5-mm-ID) sample was prepared. In some cases (carbons A, C, and D), patterns were also obtained from solid rod-shaped samples prepared for preferred-orientation measurements. For turbostratic carbons, the back-reflection diffraction peaks are too weak and broad for accurate determination of the film dimension factor. In the early stages of this work, reliance was placed on the superior dimensional stability of polyester-base film. However, experience proved this to be unsatisfactory. Film expansions as large as 0.2% were sometimes observed, compared with contractions of 0.2–0.5% for ordinary cellulose triacetate-base film. Therefore, a diamond pattern was superimposed on the carbon pattern by a separate exposure in all later experiments. Results from the solid samples were somewhat less precise than those from powder because line widths were appreciably broader and diamond patterns were generally not employed to calibrate the film dimension with these samples. No attempt was made to monitor or control the sample or camera temperature during exposure. Day-to-day variations of the room temperature by as much as ± 5°C from the normal 20°C were experienced on occasion, but during the course of an exposure (sample

*Some tendency was observed for the c values determined from various (00l) peaks to decrease with increasing l in partially graphitized carbons. Subsequent measurements with Cr, Fe, and Mo radiation indicated that this was a result of systematic reading errors caused by weak broad line, angular dependence of background, etc. In any case, the apparent dependence of c on l was in the opposite direction from that produced by absorption (which is small for carbon), and the measurable peaks occurred at relatively low angles, as noted in the text, so no extrapolation technique was applied to the powder data. In well-graphitized samples, where all the (00l) peaks could be measured with some confidence, c was independent of l within experimental error.

and standard) the variation was much less than this. In the vicinity of room temperature, the coefficient of thermal expansion of graphite parallel to the c-axis is approximately $+25 \times 10^{-6}$/°C, so that a 5°C temperature change causes c to change by only about one part in 10^4. The thermal contraction parallel to the a-axis is an order of magnitude smaller.

The degree of preferred orientation was determined by x-ray diffractometer measurements on rod-shaped samples approximately $1 \times 1 \times 10$ mm, cut parallel to the substrate. Ni-filtered Cu Kα radiation and a NaI(Tl) scintillation detector were used. The distribution of the (002) or (004) diffraction peak intensity $I(\omega)$ was measured as a function of the angle ω between the diffraction vector (bisector of the angle between the incident and diffracted beams) and the normal to the substrate plane. Tests confirmed that, within experimental error, identical results were obtained with the maximum intensity and the integrated intensity. The maximum intensity was used because it is easier to measure. The observed distribution curve was fitted graphically by the expression $I(\omega)/I(0) = \cos^n\omega$ using a log–log plot. The exponent n was used as a measure of preferred orientation. The basis for this technique has been described elsewhere (Refs. 23, 24). Alternative measures of preferred orientation are the half-width at half-maximum intensity, β, of the measured distribution; and the RMS misorientation angle $\langle\omega^2\rangle_{av}^{1/2} = \sigma$. Over the range of preferred orientations generally encountered in pyrolytic carbons, these quantities are related by the expression (Ref. 25)

$$n = 1.39\beta^{-2} = \sigma^{-2}$$

where β and σ are in radians. Preferred-orientation measurements as a function of heat treatment were made only on carbons A, C, D, and F.

The diamagnetic susceptibility of pregraphitic carbons is known to be a sensitive function of the crystallographic structure, and is a useful parameter in any study of graphitization. It depends on both L_a and c. The dependence of the total susceptibility on L_a in pyrolytic carbons was determined by measurements on a series of turbostratic as-deposited samples* on which careful determinations of L_a had been made by Fourier analysis of x-ray diffraction data (Ref. 24). It was found (Ref. 26) that the diamagnetism increased with increasing L_a, rapidly for $L_a < 200$ Å and more slowly for $L_a > 200$ Å. This curve was used to estimate the L_a values of the as-deposited carbons used in this study from their measured magnetic susceptibilities. For L_a larger than about 200 Å, the diamagnetism also increases with decreasing layer stacking order, and in turbostratic carbons may reach values 50–60% larger than the susceptibility of graphite. With increasing layer ordering, the susceptibility passes through a minimum value before finally leveling out at approximately the graphite value (Refs. 27–31). The susceptibility was measured at room temperature by the Faraday technique using a single-pan semi-microbalance and a 4-in. electromagnet with "constant-force" pole caps. An absolute calibration was obtained by determining the field gradient from a least-squares computer fit of field gradient vs distance measurements made with a 0.1% rotating-coil gaussmeter. Samples were in the form of cubes about 3 mm on a side. The susceptibility perpendicular ($\chi_\perp$) and parallel ($\chi_\parallel$) to the substrate plane was measured after each heat treatment and the total (trace) susceptibility $\chi_T = \chi_\perp + 2\chi_\parallel$, which is independent of anisotropy, was calculated. The anisotropy ratio $\chi_\perp/\chi_\parallel$ was also obtained; it is closely related to the degree of preferred orientation of the crystallites, but may differ somewhat because the intrinsic anisotropy may be a function of layer ordering.† The susceptibility perpendicular to the layer planes of the crystallite, χ_c, decreases by about 50% with the development of ordered layer stacking, while the susceptibility parallel to the layer planes, χ_a, may remain constant at the graphite value or may decrease from a higher turbostratic value. The anisotropy ratio of perfect graphite single crystals is about 68; for a large crystal of turbostratic carbon it should be near 100 if χ_a retains the graphite value, and about 70 if χ_a is also a function of layer disorder as found by Poquet (Ref. 30). Further details on the apparatus and technique employed in the susceptibility measurements have been published elsewhere (Ref. 29).

C. Heat Treatment

Heat treatments were carried out at temperatures ranging from 2400 to 3000°C in graphite tube resistance furnaces in inert gas at 1 atm. For each carbon and each treatment temperature, the susceptibility sample, the solid-rod x-ray sample (where used), and a quantity of the powdered material were loaded into a graphite crucible with a lid. All crucibles had been heated to about 3000°C and held for a minimum of 15 min prior to use, to drive off volatile impurities. Two heat-treatment techniques were used: For temperatures of 2700°C and be-

*Supplied by O. J. Guentert, Research Division, Raytheon Company.

†$(\chi_\perp/\chi_\parallel) = [2 + (n + 1)\chi_c/\chi_a]/[(n + 2) + \chi_c/\chi_a]$ where χ_c and χ_a are the principal susceptibilities parallel and perpendicular to the c-axis, respectively, and n is the preferred-orientation parameter (Ref. 23).

low, either of two identical, automatically controlled, water-cooled, low-thermal-capacity furnaces designed for creep and tensile testing was employed. Sample crucibles were loaded into a holder in the center of the hot zone. The furnace was thoroughly flushed with helium, then heated rapidly to the treatment temperature, held for the required time, and rapidly cooled by shutting off the power. Since these furnaces were not capable of sustained operation at temperatures above 2700°C, treatments at 2900 and 3000°C were carried out in a different furnace. This furnace was insulated with lamp black, was manually controlled, and had a large thermal capacity. Therefore, it was fitted with a device which allowed the samples to be rapidly inserted into the center of the hot zone from the water-cooled end of the heating element while the furnace was at the treatment temperature, and then rapidly withdrawn after the required treatment time. Since the furnace temperature commonly dropped about 50°C on insertion of the samples, the temperature was initially set high and then manually regulated to maintain the correct value during the treatment. An argon atmosphere was employed in this furnace. The sample crucibles appeared to heat to the furnace temperature within a few seconds after insertion.

In all cases, temperatures were measured with calibrated, disappearing-filament, optical pyrometers and appropriate corrections were made for window absorption. Test runs in both furnaces on crucibles with small radial holes indicated that blackbody conditions prevailed, so no emissivity correction was necessary. Ideally, the heat treatment should consist in a square pulse of temperature vs time, but in practice a finite time was required to reach the treatment temperature and there was some fluctuation of temperature during the treatment, especially in the manually controlled furnace. The nominal treatment times were therefore corrected by a procedure described in Appendix A to obtain the effective time at the specified temperature. Corrections generally amounted to less than 3 min and were therefore of negligible importance at long times, but were significant at short times. In some cases where time–temperature data were not obtained, corrections were estimated on the basis of similar recorded runs.

III. EXPERIMENTAL RESULTS

The results will be discussed primarily with reference to carbon A, on which the most complete set of data was obtained. The behavior of the other samples was in general similar to that of A and will be examined to the extent necessary to illustrate the range of behavior observed in pyrolytic carbons.

A. Unit-Cell Height

The dependence of the unit-cell height c on treatment time at various temperatures is shown in Fig. 2 for carbon A. These results were obtained with powder samples. Here c is plotted against the logarithm of the total treatment time. It is evident that layer ordering is a strong function of both time and temperature of treatment. Furthermore, the graphitization process is seen to occur by a succession of distinct stages in this carbon. Two stages are illustrated in Fig. 2. In Stage I, c decreases from an initial as-deposited value of about 6.85 Å to a plateau at about 6.74 Å; in Stage II there is a further decrease to about 6.72 Å. Presumably, at sufficient long times there would be a third stage in which c would decrease to the graphite value of 6.708 Å. This third stage has not been observed in the present investigation, but good evidence for it exists from isochronal heat-treatment experiments at temperatures above 3000°C (Refs. 32, 33).

Stages I and II have the form of single first-order rate processes* with rate constants differing by about a factor of 30. The experimental data corresponding to any treatment temperature can be represented quite well by the simple sum of two first-order rate terms in Eq. (1)

*The present data are neither detailed nor precise enough to establish with certainty that graphitization is a first-order process. However, first-order equations fit the data very well. It is convenient to discuss the results from this standpoint.

$$c = c_2 + (c_0 - c_1)\ \exp(-k_1 t) + (c_1 - c_2)\exp(-k_2 t). \quad (1)$$

Here c_0, c_1, and c_2 are the initial, end of Stage I, and end of Stage II values, respectively, of the unit-cell height; k_1 and k_2 are rate constants; and t is the total treatment time at that temperature. For carbon A, $c_0 \simeq 6.85$ Å, $c_1 \simeq 6.74$ Å, and $c_2 \simeq 6.72$ Å. The points in Fig. 2 represent the experimental data, but the curves represent Eq. (1). The only parameters that have been changed to fit data at different temperatures are the rate constants k_1 and k_2. All of the data could be superimposed on a single curve of the type given by Eq. (1) simply by translation along the log time axis [this is equivalent to scaling the time for each curve by a factor $K(T)$]. This feature will be used later in the determination of the activation energy. It may be noted here that this constitutes strong evidence that the graphitization process is the same regardless of the treatment temperature; apparently, exactly the same results could be obtained at a treatment temperature of 2400°C, with sufficiently long treatment times (of the order of one year), as are realized at 3000°C in half an hour.

The simple two-stage kinetic behavior illustrated in Fig. 2 was observed for most of the carbons studied. Carbons A–E all followed this general pattern. Within the limitations of the relatively small number of examples studied, it appears that this kinetic behavior is typical of substrate nucleated carbons deposited under the usual conditions. All of these carbons had moderately large as-deposited apparent crystallite diameters ($L_a \simeq 200$–350 Å). However, graphitization rates at any given temperature differed by about a factor of ten within this group. Carbon A was the fastest and carbon B was the slowest, as shown in Fig. 3. Here unit-cell height vs log

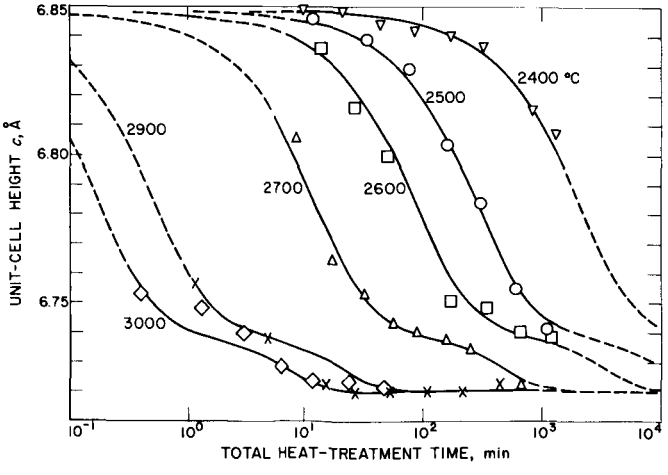

Fig. 2. Unit-cell height as a function of log treatment time at several temperatures for carbon A; points, experimental data; curves, Eq. (1)

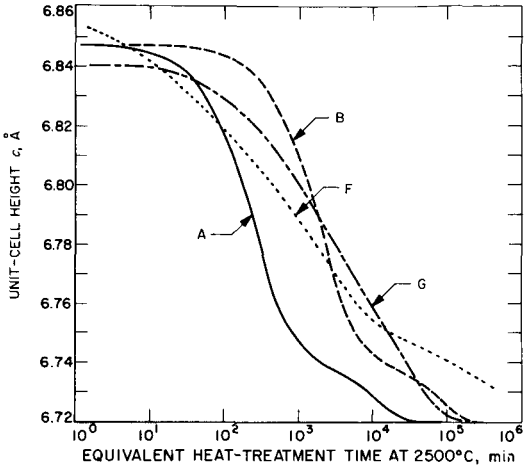

Fig. 3. Unit-cell height as a function of log treatment time at 2500°C for several carbons

time curves at 2500°C for several carbons are compared (these curves were extended beyond the range of treatment times actually employed at 2500°C by superposition of data obtained at other temperatures, as will be described later). Variations in rate were also observed in samples taken from different locations in the same deposit (cf. D_1 and D_2 in Fig. 15). Carbon F, with a regeneratively nucleated structure and $L_a \approx 240$ Å, had a somewhat broader kinetic response than carbons A–E, but still showed distinct stages. The structure at the end of Stage II, with $c \simeq 6.74$–6.76 Å, appeared to be unusually stable in the regenerative structure. Carbon G, deposited at 1800°C with a very coarse substrate nucleated structure and a fairly small L_a value of ~150 Å, also exhibited a broadened kinetic curve, and here two stages were not resolved. The kinetic behavior of carbons F and G cannot be satisfactorily represented by Eq. (1). It is necessary to employ a superposition of many first-order terms with a fairly narrow distribution of rate constants, $f(\ln k)$

$$c = c_2 + (c_0 - c_2)\int_{-\infty}^{+\infty} f(\ln k)\exp(-kt)\, d\ln k \quad (2)$$

For carbon F, $f(\ln k)$ has two peaks corresponding to Stages I and II, while for carbon G the distribution has a single broad peak.

These unit-cell results were obtained on annealed powder samples, while the magnetic-susceptibility and

preferred-orientation measurements described below were obtained on solid samples. Possible influences of sample size on graphitization behavior were investigated as discussed in Appendix B. It was found that there was no appreciable effect for the range of sample sizes ($\sim 40\mu$ powder to 3-mm cubes) used here.

B. Diamagnetic Susceptibility

The change in total diamagnetic susceptibility χ_T as a function of heat-treatment time at various temperatures is shown in Fig. 4 for carbon A. Again, two-stage behavior

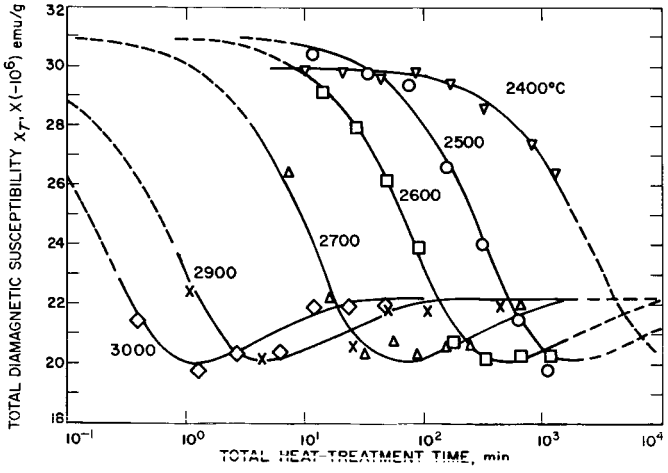

Fig. 4. Total diamagnetic susceptibility as a function of log treatment time at several temperatures for carbon A; points, experimental data; curves, Eq. (3)

is evident. During the first stage χ_T decreased from its initial high as-deposited value to a minimum value of about 20*; during the second stage, χ_T recovered toward the graphite value of 22. In Fig. 4 the points represent the experimental data while the curves were computed from Eq.(3):

$$\chi_T = \chi_{min} + (\chi_0 - \chi_{min}) \exp(-k_1 t) + (\chi_\infty - \chi_{min})[1 - \exp(-k_2 t)] \quad (3)$$

where χ_0 is the initial (as-deposited) total diamagnetic susceptibility, χ_{min} is the minimum (end of Stage I) total diamagnetic susceptibility, and χ_∞ is the final (graphite) total diamagnetic susceptibility; the other quantities are as defined earlier. For carbon A, χ_0 varied from 29 to 31 for different samples, $\chi_{min} \simeq 19.8$ and $\chi_\infty \simeq 22$. This behavior was typical of carbons A–E, although χ_0 varied over the range 29 to 33 and although there was a range of about 10 for the rate constants for the various carbons at the same treatment temperature, as already noted for the unit-cell height results. Carbon F had a somewhat broader kinetic response and the susceptibility did not recover from the minimum value with the heat-treatment schedule employed here. However, isochronal treatments at temperatures above 3000°C did cause χ_T to increase toward the graphite value. For carbon G, the as-deposited susceptibility was low (21–22), and initially increased as a function of heat-treatment time to a maximum value of about 24 before going through the minimum.

The close correlation between χ_T and c is shown in Fig. 5. The upper curve shows representative data for carbons A–F, while the lower curve refers to carbon G.

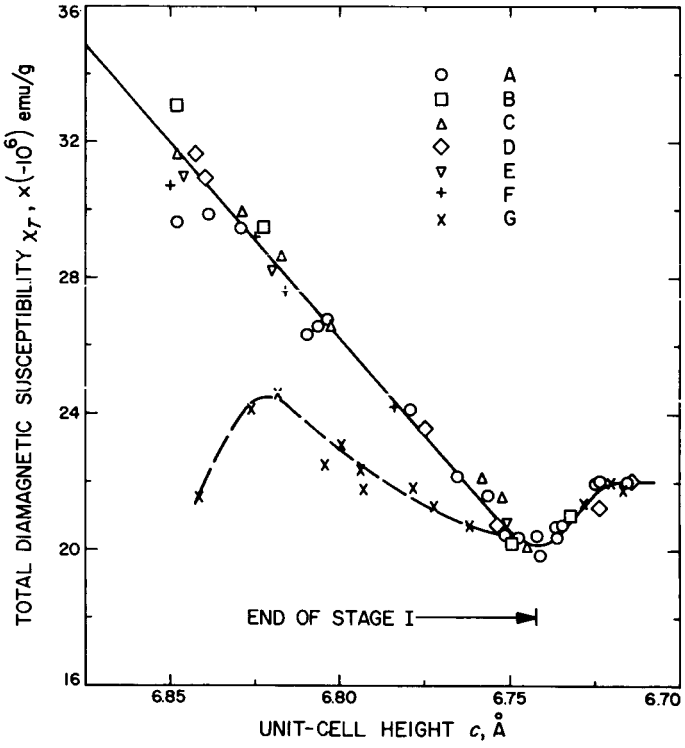

Fig. 5. Total diamagnetic susceptibility as a function of unit-cell height for several carbons

Decreasing susceptibility results from increasing layer stacking order (Refs. 27, 29–31), while increasing susceptibility can be attributed to increasing L_a (Refs. 26, 27). The susceptibility minimum occurs at the end of the Stage I decrease in unit-cell height (i.e., at $c \simeq 6.74$–6.75 Å) and is a result of the combination of these two

*All susceptibility values are expressed in units of (-10^{-6}) emu/g.

processes. The form of the curve for carbons A–F indicates that there is little change in L_a during Stage I, but L_a increases during Stage II in these carbons. The behavior of carbons A–F appears to be characteristic of pyrolytic carbons deposited under the usual conditions ($L_a \simeq 200$–350 Å). The somewhat different behavior of carbon G is evidently associated with its smaller as-deposited L_a of ~ 150 Å. The initial susceptibility increase indicates that L_a increases during the early as well as the later stages of graphitization in this carbon.

The susceptibility anisotropy ratio ($\chi_\perp/\chi_{||}$) is shown as a function of treatment time at various temperatures for carbon A in Fig. 6. The anisotropy ratio is related to the degree of preferred orientation (alignment of the basal planes of the crystallites parallel to the substrate).

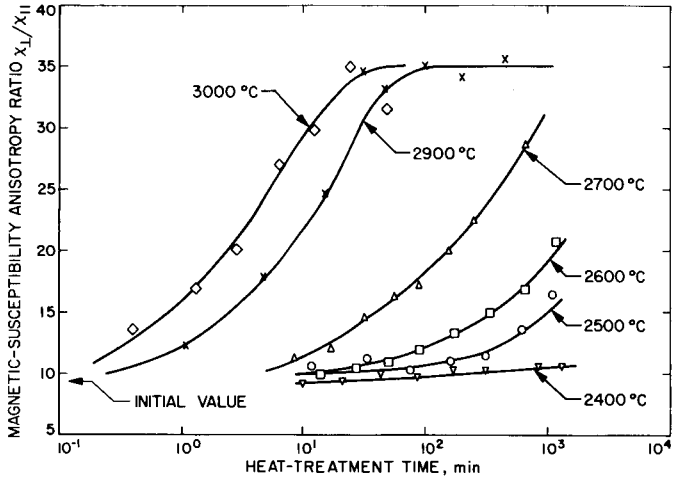

Fig. 6. Diamagnetic-susceptibility anisotropy ratio as a function of log treatment time at several temperatures for carbon A

This parameter is also a strong function of both the time and temperature of treatment. In Fig. 7 the value of the anisotropy ratio after the final heat treatment at each temperature is plotted against c for several carbons. Little change in anisotropy ratio occurs during Stage I, but there is a rapid increase during Stage II and III.

C. Preferred Orientation (x-ray)

The anisotropy ratio results indicate that the degree of preferred orientation tends to increase when pyrolytic carbons are heat-treated. A plot of the preferred-orientation parameter n against the logarithm of the treatment time at several temperatures is shown in Fig. 8 for carbon A. It is possible to represent these data

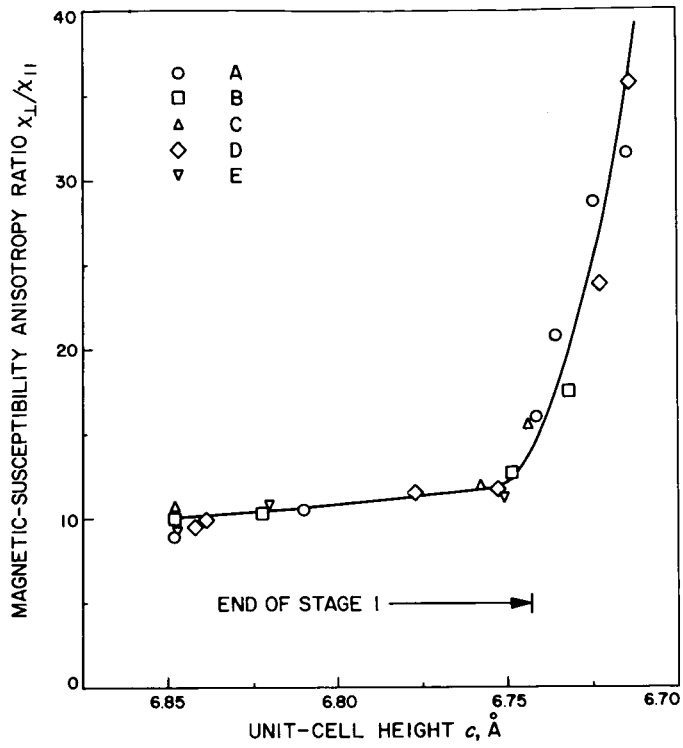

Fig. 7. Diamagnetic-susceptibility anisotropy ratio as a function of unit-cell height for several carbons

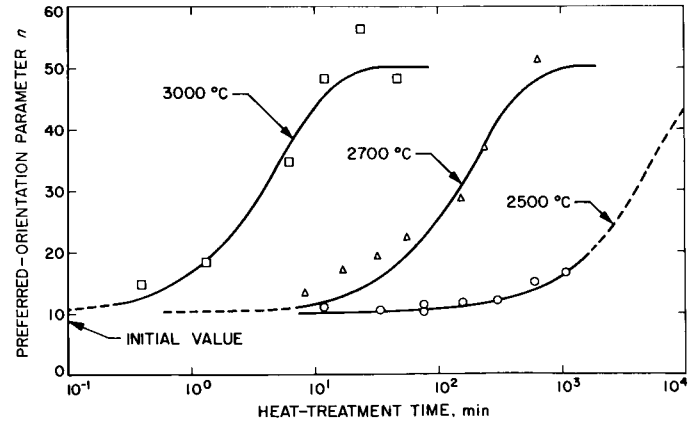

Fig. 8. Preferred-orientation parameter as a function of log treatment time at several temperatures for carbon A; points, experimental data; curves, Eq. (4)

approximately with a single first-order rate term as shown by the solid curves in Fig. 8:

$$n = n_0 + (n_\infty - n_0)\,[1 - \exp(-k_2' t)] \qquad (4)$$

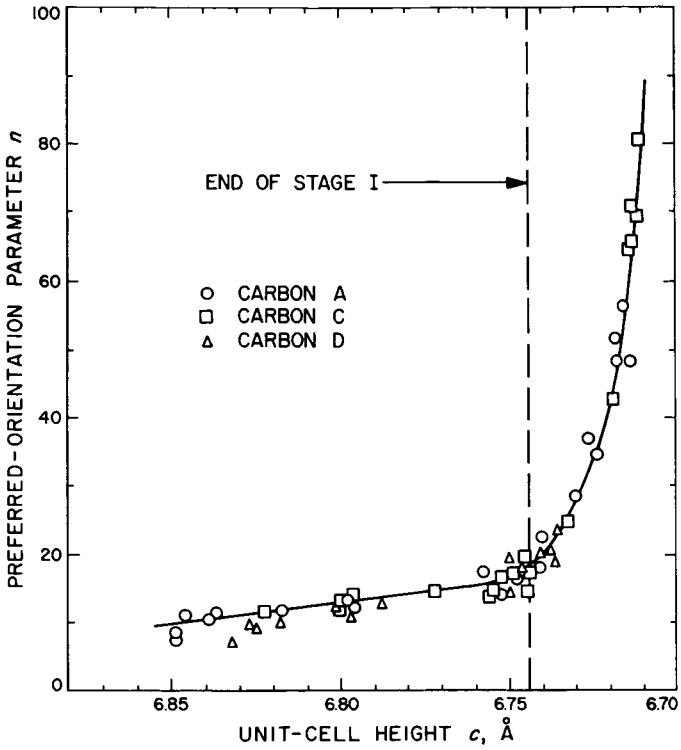

Fig. 9. Preferred-orientation parameter as a function of unit-cell height for several carbons

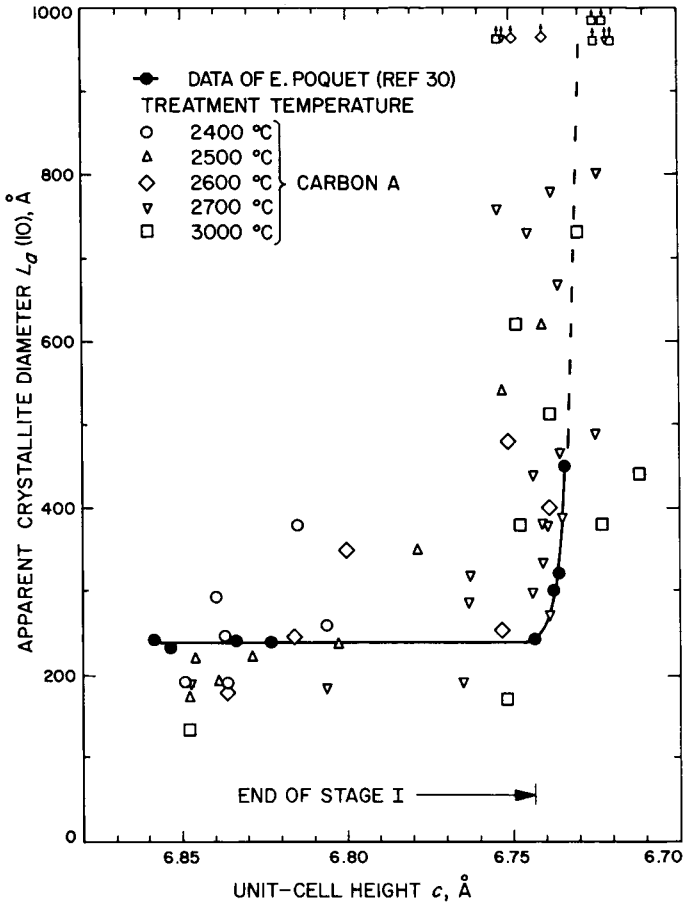

Fig. 10. Apparent crystallite layer diameter (x-ray) as a function of unit-cell height for two carbons heat-treated at various temperatures

where n_0 and n_∞ are the initial (as-deposited) and final values, respectively of the preferred-orientation parameter; t is total treatment time and k_2' is the rate constant. It will be shown later that this k_2' is approximately the same as k_2 in Eqs. (1) and (3). There is some increase in preferred orientation during Stage I, but most of the increase occurs during the later stages. This is illustrated in Fig. 9, where n values for three carbons (A, C, and D) are plotted against unit-cell height. It is interesting that the values for all three of these carbons fall on the same curve. A few preferred-orientation measurements were also taken on carbon F. The initial n value for this material was somewhat lower than for the substrate nucleated carbons and only a slight increase was observed even after 350 min at 2900°C. This illustrates again the relative stability of the regenerative structure.

D. Apparent Crystallite Diameter (x-ray)

Only qualitative information about L_a can be obtained from magnetic-susceptibility measurements on partially graphitized carbons because of the influence of layer ordering on the susceptibility. Therefore, approximate values of L_a were determined by the x-ray diffraction peak-displacement method, as described in Section II above, after various heat treatments. The results for carbon A are shown as a function of interlayer spacing in Fig. 10. Although the data points scatter badly, it is clear that there is little or no increase in L_a during Stage I, but pronounced crystallite growth occurs during the later stages, consistent with the magnetic behavior. These crude results are in good agreement with the much more precise isochronal data of Poquet (Ref. 30) on a similar pyrolytic carbon, which are also shown in Fig. 10. Since Poquet's measurements were made by the more general peak profile method, this agreement implies that Warren's formula relating L_a to the (hk) peak displacement is not limited to turbostratic carbons, but may also be used to estimate the apparent crystallite diameter in partially graphitized carbons as well by using the $(hk0)$ peak.

E. Microstructure

A few observations have also been made on the effect of heat-treatment time and temperature on the micro-

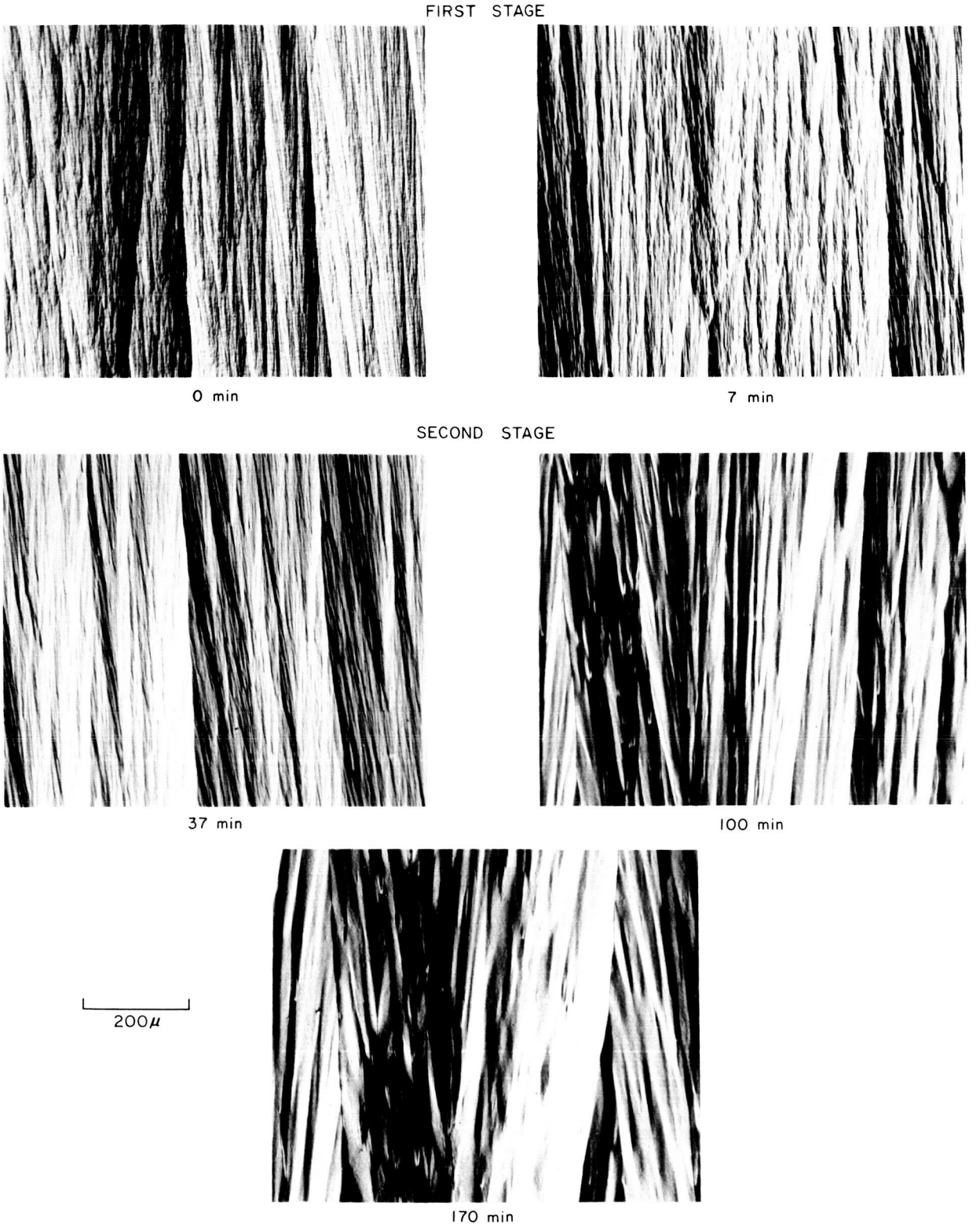

Fig. 11. Microstructures after increasing isothermal treatment times at 2900°C for carbon D

structure of pyrolytic carbons. It has been found that there is very little change in microstructure, as observed with an optical microscope and polarized light, during the first stage of graphitization. However, during the second stage the fine structure within the growth cones begins to disappear, producing a coarsening of the structure. This is illustrated by the sequence of micrographs in Fig. 11, in which the effect of isothermal heat treatment at 2900°C on carbon D is shown. The contrast in these polarized-light micrographs is a result of varying basal-plane orientations. Isochronal heat-treatment experiments at temperatures above 3000°C show that, with increasing treatment beyond the end of the second-stage region (i.e., Stage III), the cone structure largely disappears and only traces of the major cone boundaries remain. This is shown in Fig. 12 for carbons E and F. Again it is evident that the regenerative-type structure of carbon F is much more stable than the substrate nucleated structure represented by carbon E.

F. Dimensional Changes

Pyrolytic carbons undergo an irreversible change in macroscopic dimensions as a result of the structural changes which occur during heat treatment. It should be expected that such dimensional changes would occur primarily during Stages II and III. No data on this aspect of the transformation were obtained in this investigation, but examination of published data confirms that this is so, as discussed in Appendix C.

G. Activation Energy for Graphitization

The results described in the preceding sections show that the structure and properties of pyrolytic carbons change as a function of isothermal heat-treatment time, and the rate of change increases rapidly with increasing treatment temperature. These are the general characteristics of a thermally activated process. Therefore, it may be expected that the rate constants in Eqs. (1)–(4) will exhibit an Arrhenius-type dependence on treatment temperature

$$k = k_0 \exp(-\Delta H/RT) = k_0 K(T) \qquad (5)$$

where ΔH is an activation energy, R is the gas constant, T is the absolute temperature, k_0 is a constant independent of temperature, and $K(T) = \exp(-\Delta H/RT)$ is the Boltzmann factor.

Several techniques are available for determining the effective activation energy. In principle, for a process described by a single first-order rate term, the rate constant at each temperature can be determined by plotting the fractional change in the measured property [$(c - c_2)/(c_0 - c_2)$, for example] on a logarithmic scale against time. The slope of this curve is the rate constant k. Data for carbon A have been plotted in this manner in Fig. 13. For a sum of two first-order terms, the asymptotic slope at long times ($t >> 1/k_1$) is k_2, while the slope at very short times ($t << 1/k_2$) is k_1. When the k values are known, ΔH may be determined in the usual way using Eq. (5) as shown in Fig. 14. For proper application, this method requires a large number of data points linearly distributed on the time scale; the method is quite sensitive to data scatter. In effect, the data points at very long and very short times are heavily weighted with respect to those at intermediate times in the present case. This method is not appropriate at all in cases where there is a distribution of unresolved rate processes. While this method of analysis may be applied to much of the present data, as illustrated in Fig. 13, other methods are more suitable. The methods of curve fitting and data superposition described below are entirely equivalent to the above technique and have the advantages of simplicity, full use of all data points, and relative insensitivity to data scatter. In addition, the superposition method may easily be applied to cases where there is a distribution of rate constants, such as carbons F and G.

Where Eqs. (1), (2), or (4) have been fitted to the data (as for carbon A), appropriate values of k_1 and k_2 are determined in the fitting process. These rate constants for carbon A are plotted on a logarithmic scale against reciprocal absolute temperature in Fig. 14. The k_1 values determined from the plot in Fig. 13 are also shown. It is evident that Eq. (5) is obeyed very well. Therefore, the graphitization of pyrolytic carbons may be considered to be a thermally activated process with a temperature-independent effective activation energy, at least in the temperature range 2400–3000°C investigated here. The rate-constant values determined from unit-cell height and magnetic-susceptibility data agree very well with each other. For both Stages I and II the effective activation energy determined from the Fig. 14 plot is ~270 kcal/mole. The more limited k_2' data obtained from the preferred-orientation data fall very close to the k_2 data from c and χ_T. This result may be expected from the fact that n is a function of c (Fig. 9) and is further evidence that the preferred-orientation increase is associated with the second stage of graphitization. The best straight line through the k_2' points corresponds to $\Delta H \sim 250$ kcal/mole. Within experimental accuracy this value may be considered equivalent to the 270 kcal/mole value for c and χ_T.

An alternative technique for determining the activation energy is the method of superposition. Consider the

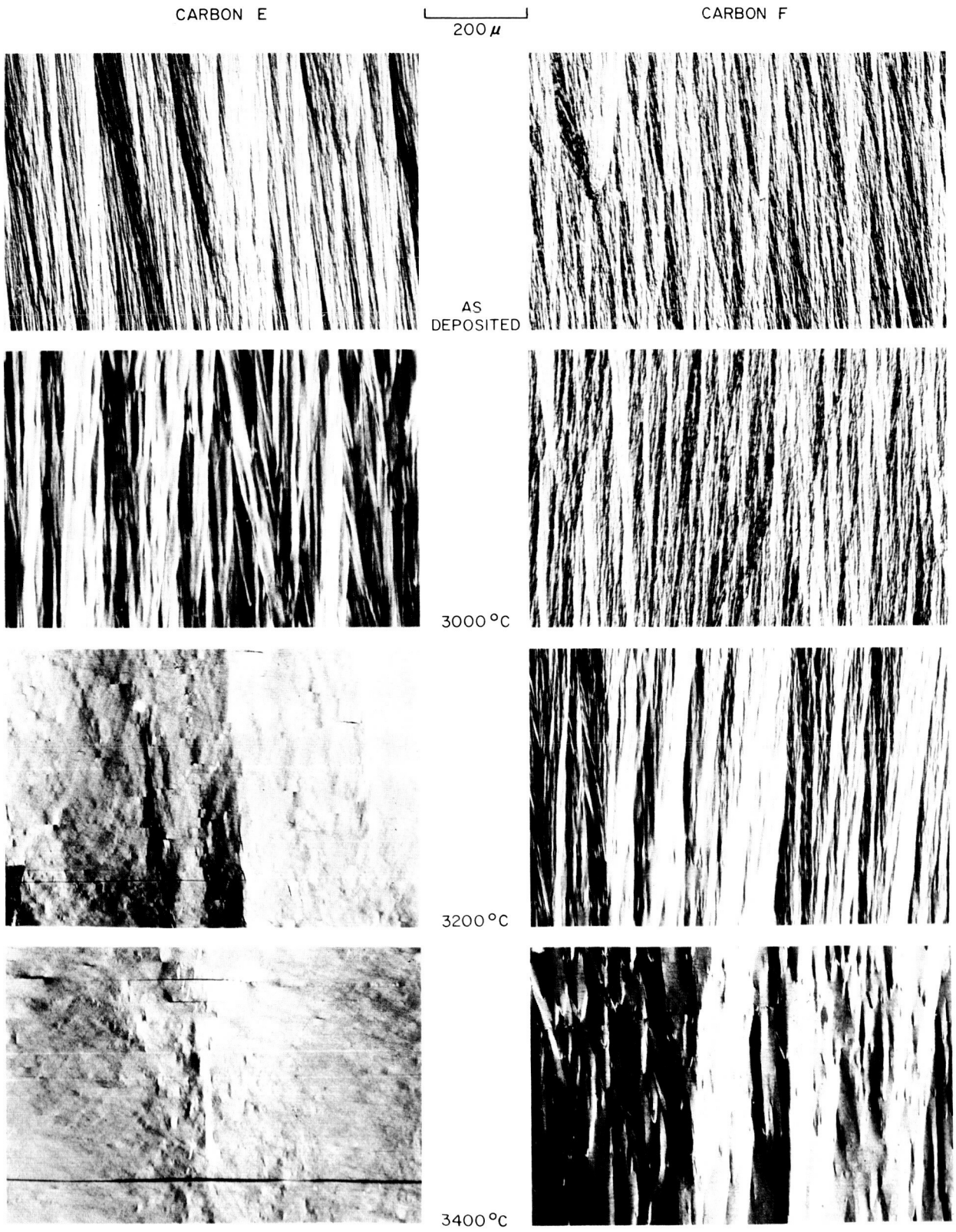

Fig. 12. Microstructures after isochronal (15–30 min) heat treatments at increasing temperature for carbons E and F

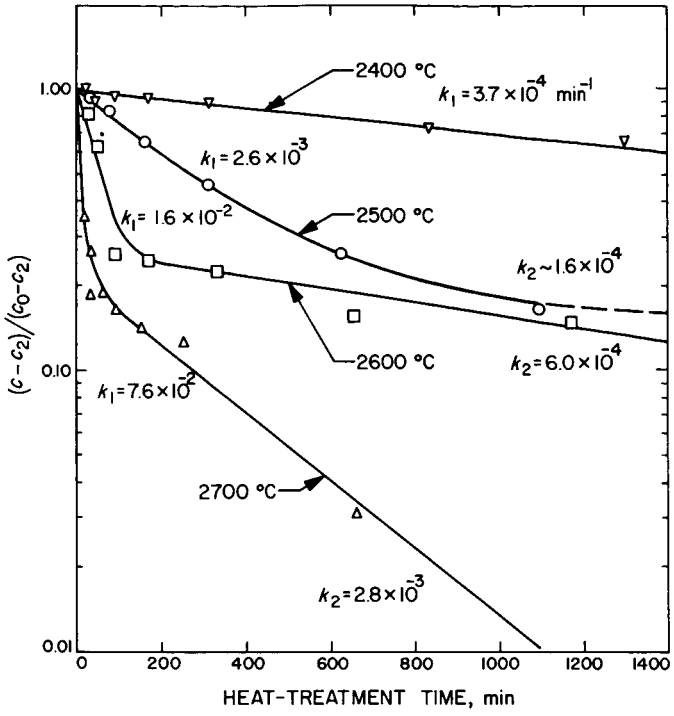

Fig. 13. Fractional change in unit-cell height (logarithmic scale) as a function of treatment time at various temperatures for carbon A

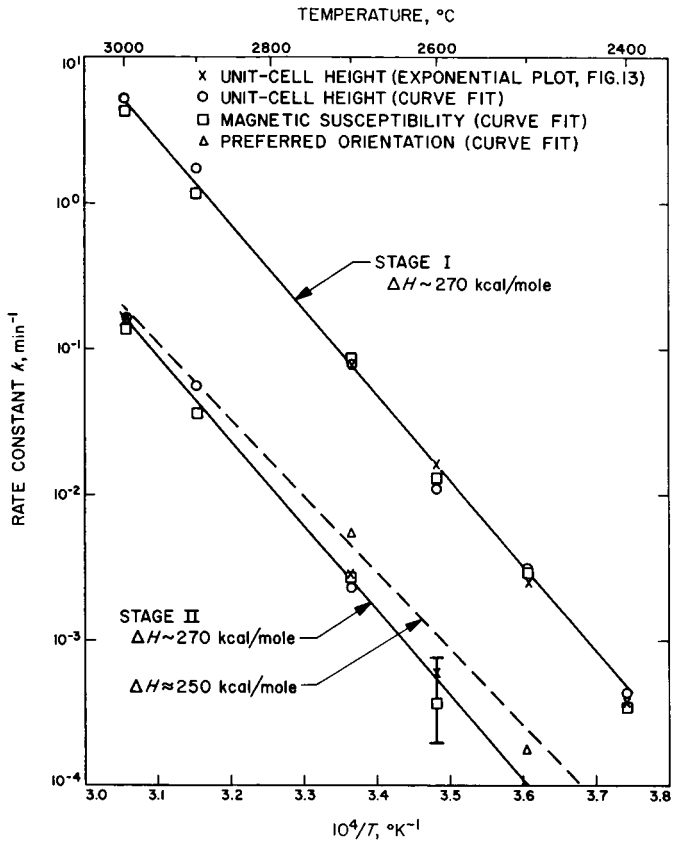

Fig. 14. Arrhenius plot of rate constants for carbon A

unit-cell height data, for example. If Eqs. (1) and (5) are good representations of the data, then the Stage I portion of the c vs log t plot at temperature T differs from that at an arbitrary reference temperature T_0 only by a scale factor $K(T)/K(T_0)$ on the time scale. Therefore, it should be possible to superimpose all of the Stage I data on a single curve (corresponding to a treatment temperature T_0) simply by translation parallel to the log t axis. Then,

$$\ln [K(T)/K(T_0)] = \ln t_0 - \ln t = -(\Delta H/R)(1/T - 1/T_0) \quad (6)$$

and the effective activation energy may be determined from the dependence of $(\ln t_0 - \ln t)$, the amount each curve must be displaced to cause superposition, on the reciprocal of the absolute temperature. Similar arguments apply to Stage II, and to the χ_T and n data as well. It can be shown that the superposition technique also can be applied where there is a broad distribution of rate constants if the distribution function is independent of temperature. This is assured if both k_0 and ΔH are independent of temperature (Ref. 34). When this method was applied to the present data, it was found that the curves corresponding to various treatment temperatures superimposed very nicely. The same translation along the log t axis superimposed both the Stage I and Stage II portions of the curve within experimental uncertainty, indicating that the effective activation energy is the same for both stages (as already found from the curve-fitting results on carbon A). The effective activation-energy value determined in this way for carbon A is 272 kcal/mole, in very good agreement with the value determined from the rate constants (Fig. 14). This technique has been applied to data from all seven of the pyrolytic carbons investigated, as shown in Fig. 15. For clarity, the curves have been displaced along the ordinate axis (corresponding to taking a different value of T_0 for each carbon). The ΔH values determined by a linear least-squares fit are as follows, in kcal/mole: A, 272; B, 251; C, 247; D_1, 279; D_2, 273; E, 255; F, 261; and G, 247. Samples D_1 and D_2 were taken from different locations of the same deposit. The average ΔH value is 261 kcal/mole.

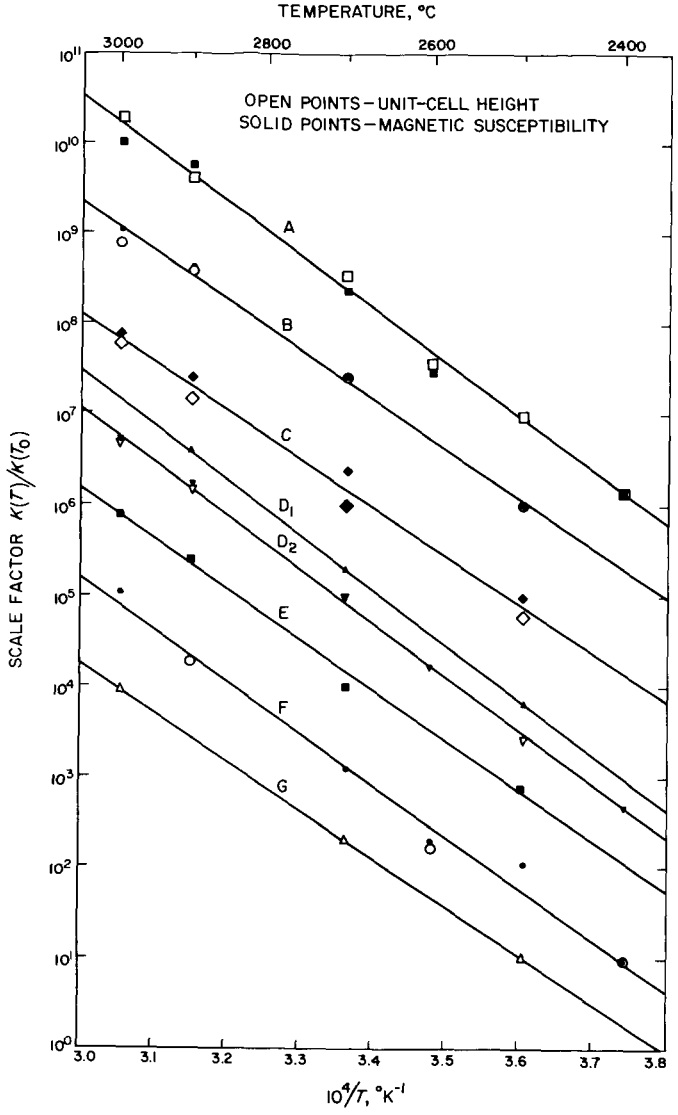

Fig. 15. Arrhenius plot, obtained by superposition method, for various carbons

IV. DISCUSSION

It has been reported (Ref. 13) that the degree of graphitization of pyrolytic carbons approaches a limiting "saturation" value which increases with increasing isothermal treatment temperature, after a relatively short (1 hr) treatment time. It has also been reported, on the basis of isochronal heat-treatment experiments, that there is a well-defined graphitization temperature for pyrolytic carbons (Ref. 14). The results presented in the preceding sections demonstrate clearly that neither of these concepts is valid for the seven representative pyrolytic carbons investigated here. The graphitization of these carbons is a thermally activated kinetic process and thus depends strongly on both time and temperature of treatment. Furthermore, no apparent change in the effective activation energy or kinetic mode of transformation with treatment temperature is evident, and identical results

can be obtained over a wide temperature range if the treatment time scale is properly adjusted. However, it is easy to understand how such misconceptions about the kinetics of graphitization could arise. When considered in terms of a linear time scale, the continuing isothermal increase in graphitization is not nearly so obvious, especially if there is some scatter in the data or the degree of graphitization is assessed qualitatively (as in Ref. 13). If vertical cuts are made on Fig. 2, it is evident that for any isochronal annealing period there will be a fairly sharp apparent "graphitization temperature" (e.g., about 2700°C at 30 min). However, this "critical" temperature will decrease as the treatment time is increased (e.g., to about 2500°C at 600 min), and will vary from one lot of pyrolytic carbon to another. The relative sharpness of this fictitious temperature is a result of the high effective activation energy.

The multistage mode of transformation is a striking feature of the kinetic behavior of carbons A–F. The first stage is characterized by a large increase in layer ordering with little change in the other structural parameters. Later stages are characterized by large increases in crystallite size and preferred orientation, and by microstructural and dimensional changes. The close correlation of the apparent crystallite layer diameter (L_a) and the degree of preferred orientation (n and $\chi_\perp/\chi_\parallel$) with unit-cell height c in these carbons, especially in the second stage of graphitization, is noteworthy (Figs. 7, 9, and 10). Of the two variables, L_a has been cited most frequently in the literature as an important parameter in the graphitization process, but the significance of preferred orientation has also been recognized. Therefore, the relationship of each of these parameters to the graphitization process in pyrolytic carbons must be considered.

Studies on the graphitization of carbon blacks suggest that the attainable degree of layer ordering is an increasing function of L_a. In these carbons the maximum L_a is limited by the small particle size. It is observed that the smallest blacks are essentially nongraphitizing, while an increasing amount of layer ordering can be achieved in blacks of increasing particle size (Refs. 35, 36). A strong correlation between c and L_a has been noted for conventional soft carbons as well as blacks by Mering and Maire (Refs. 37, 38) and by Takahashi, Kuroda, and Akamatu (Ref. 39). The latter three suggested that the relationship could be expressed analytically in the form

$$c = 6.708 + 19/L_a \qquad (7)$$

Assuming that a relationship similar to Eq. (7) is valid for pyrolytic carbons, the multistage kinetic behavior of carbons A–F can be understood as depicted schematically

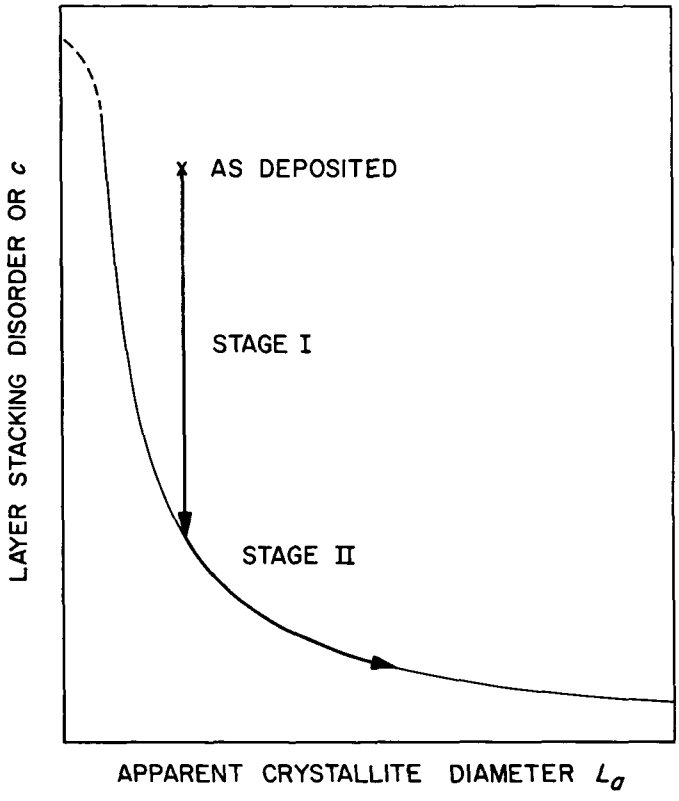

Fig. 16. Schematic representation of the degree of layer stacking disorder as a function of apparent crystallite diameter (light line) showing the graphitization path followed by many pyrolytic carbons (heavy line)

in Fig. 16. In the as-deposited condition, the unit-cell height (6.85 Å) is much larger (and the layer ordering much less) than the "equilibrium" value corresponding to the large L_a value (220–350 Å). Therefore, initially layer ordering occurs at essentially constant L_a. This is Stage I. After the degree of layer ordering corresponding to the as-deposited L_a value is reached, further ordering (Stage II and beyond) must await crystallite growth. Thus L_a and layer ordering increase simultaneously during the later portions of the graphitization process. The rate-determining process in Stage I is layer ordering; in later stages it is evidently crystallite growth, which may reasonably be assumed to be a slower process. For carbon G the as-deposited L_a is smaller ($\sim$150 Å), placing it near the steeply rising portion of the equilibrium curve in Fig. 16. Stage I, if it exists at all, will be small and difficult to resolve, and L_a will begin to increase early in the graphitization process as observed. The multistage behavior of the susceptibility can similarly be understood in terms of the dependence of the magnetic properties

of L_a and c, as discussed earlier. The reason for the existence of more than two stages of graphitization is not clear, but Stage III may be associated with residual cone boundaries and other structural defects which remain at the end of Stage II and which are difficult to anneal out. The microstructures (Figs. 11 and 12) provide direct support for this possibility.

The differences in Stage I rate constants for different carbons and the distribution of rate constants found in carbons such as G and F also appear to be related to L_a. Values of the Stage I rate constant k_1 at 2500°C and of as-deposited L_a values for several of the carbons are tabulated in Table 2. These data can be arranged in an ordered sequence with the L_a values increasing monotonically with decreasing k_1 values, as shown. An order-of-magnitude decrease in k_1 appears to be associated with an L_a increase of about 40%.

Table 2. Correlation between Stage I rate constant k_1 and apparent crystallite diameter L_a determined from total diamagnetic susceptibility χ_T (as deposited)

Carbon	k_1 (2500°C), min^{-1}	χ_T, -10^{-6} emu/g	L_a, A
A	3.2×10^{-3}	30 ±1	~240
C	$\sim 1.7 \times 10^{-3}$	31.6 ±1	~280
D	$\sim 1.3 \times 10^{-3}$	31.7 ±0.7	~280
E	$\sim 6 \times 10^{-4}$	32.0 ±1	~290
B	2×10^{-4}	33.1 ±0.4	~340

It is appropriate here to digress briefly from the discussion of the experimental results to consider the significance of L_a. This quantity is usually determined from the widths of the (hk) or ($hk0$) x-ray diffraction peaks, or—better—from Fourier analysis of their profiles. However, line broadening may be produced by lattice distortion as well as by small crystallite size. It is very difficult to separate these two components of the peak broadening. An appreciable distortion contribution is present in the L_a values determined by the usual techniques for most conventional carbons. This is indicated by the fact that the L_a values determined from different diffraction peaks generally differ appreciably. The quantity L_a may be considered most generally as a coherent diffraction length which is a function of both the true crystallite diameter and lattice distortion such as bending. For this reason the term *apparent crystallite diameter* has been applied to L_a by Mering and Maire (Ref. 37) and is used here. However, Guentert (Ref. 24) found that, for a number of pyrolytic carbons deposited at 2000°C and above, the L_a values determined by Fourier analysis of the (10) and (11) peaks differed by only 10% or less. This difference is probably within the error limits of the measurement in this L_a range (greater than 200 Å). Therefore, it appears that in these materials distortion may not be a serious problem and L_a may be considered to represent (or at least be proportional to) the actual average crystallite layer diameter in pyrolytic carbons such as A–F.

Now the role of preferred orientation in the graphitization process may be examined. The close correlation between L_a and preferred orientation observed here (compare Fig. 9 with Fig. 10) might have been anticipated, especially for a dense, highly textured structure such as that of pyrolytic carbon. Parallel alignment of adjacent crystallites will obviously facilitate crystallite growth. Under certain conditions, such as the removal of tilt boundaries or the flattening of curved layers, an increase in preferred orientation corresponds directly to an increase in apparent crystallite diameter. The primary source of the driving energy for the preferred-orientation increase on treatment at high temperatures is differential thermal expansion (Ref. 40). The thermal expansion of turbostratic and graphite crystallites is highly anisotropic and this anisotropy is not very sensitive to layer ordering. The linear-expansion coefficient normal to the layer planes is about 25×10^{-6}/°C near room temperature and increases at high temperatures, while parallel to the layers there is an initial small contraction at moderate temperatures and an expansion of about 1×10^{-6} at high temperatures (Refs. 40–42). The influence of preferred orientation and differential thermal expansion on crystallite growth in conventional carbons has been discussed by Tsuzuku (Ref. 43), Mizushima (Ref. 44), and Akamatu and Kuroda (Ref. 45). For pyrolytic carbons, at temperatures appreciably above or below the deposition temperature this expansion anisotropy produces high internal stresses in the imperfectly oriented polycrystalline carbon. At low temperatures these stresses are frozen in. At high temperatures (say above 2300°C) atomic diffusion and plastic deformation can occur, and the internal stresses can be relieved by structural changes which result in increased preferred orientation. If all of the crystallites have their c-axes parallel, there is no thermal expansion stress in a uniformly heated, unconstrained flat plate. Because of the influence of preferred orientation on crystallite growth, the actual rate-determining process for the second stage may be the preferred-orientation increase.* The behavior of carbon F

*The lack of any appreciable influence of sample size on second-stage graphitization would seem to provide some evidence against this hypothesis. However, the powder particle size (~40μ) is appreciably larger than the subcone size seen in the micrographs and it is primarily these subcone boundaries which anneal out during Stage II (Fig. 11). The particle size is two to three orders of magnitude larger than the crystallite size (200 to ≈1000 Å) in this stage of graphitization.

(regenerative microstructure) is instructive in this regard. Very little preferred-orientation increase occurs and Stage II graphitization is inhibited in this carbon.

The difference in rates between Stages I and II, the range in rates for different pyrolytic carbons, and the distribution of rates in carbons such as G could be associated with either or both of two parameters in the Arrhenius equation (5): the activation energy ΔH and the pre-exponential factor k_0. These parameters can be discussed with confidence only when the nature of the activated process is understood in some detail. This understanding has not yet been achieved for carbons and graphite, and the observed ΔH value is therefore best considered an effective or apparent activation energy. Nevertheless, some useful inferences may be drawn from the results reported here.

Because of the small range of rate constants which can conveniently be measured as a function of temperature, k_0 is very difficult to determine experimentally with any precision. On the other hand, if k_0 is known from theory, a more reliable value for ΔH may be obtained by fitting the Arrhenius plot to k_0 (Ref. 46). Unfortunately, no k_0 value is available for the present case. Theoretical calculation, difficult at best, is precluded by lack of knowledge of the detailed nature of the thermally activated process involved. Calculation of the effective activation energy by the superposition method does not yield a value for k_0, but it can be determined from the rate constants. If it is assumed that k_0 is the same for Stages I and II and is given by extrapolation of the more extensive Stage I data ($k_0 \approx 5 \times 10^{16}$ sec^{-1} for carbon A), the apparent activation energy for Stage II is increased by only about 30 kcal/mole (i.e., to ~300 kcal/mole) for carbon A. The spread and distribution in Stage I rates observed in other pyrolytic carbons could be accounted for in terms of a similarly small range of ΔH values. However, when the kinetics of graphitization of conventional carbons are examined, it is found that a large range of activation energy values is required to account for the observed behavior on this basis (Refs. 2, 4). On the other hand, if it is assumed that ΔH is constant and that there is a distribution of k_0 values, an effective activation energy is obtained for these carbons which is in excellent agreement with the pyrolytic-carbon value (Refs. 18, 47, 48). Thus, a distribution of pre-exponential factors yields a more consistent interpretation of graphitization kinetics than does a distribution of activation energies.

It has been shown earlier that both k_1 and k_2 appear to depend on microstructural parameters, especially L_a. It is difficult to see why the activation energy should depend on the microstructure in this manner, but k_0 could easily be structure-sensitive. An incomplete but instructive analogy may be found in the annealing of excess point defects in metals introduced by irradiation or quenching. Consider, for example, the effect of single vacancies on the electrical resistivity. As a vacancy migrates through the crystal lattice, the resistivity increment which it produces remains unchanged until the vacancy disappears at a sink or combines with other defects. The activation energy observed for annealing of the resistivity will be that for vacancy migration. The pre-exponential factor will be a function of the average lifetime (number of jumps) of the vacancy. It will depend on the microstructure of the sample and other experimental parameters. The progress of graphitization is measured experimentally by observing a macroscopic variable, such as average unit-cell height or diamagnetic susceptibility, which depends on layer ordering. To produce a change in the measured variable, one or more layer planes in at least one crystallite must move from a disordered to an ordered position by a thermally activated process. It is reasonable to assume that the fundamental, thermally activated process is a one-atomic-distance jump of a single atom. It is very unlikely that a single atomic jump can accomplish layer ordering, however. Rather, a large number of atomic jumps must occur to permit even a single layer-plane to take an ordered position relative to neighboring planes. Then k_0 will be a function of this number of jumps. As will be discussed later, the required number of atomic jumps can reasonably be expected to be a function of the size of the ordering plane and the nature of its peripheral attachment to neighboring crystallites. Therefore, k_0 should be a function of the microstructure. For these reasons, it is the author's conviction that the graphitization process in pyrolytic and other soft carbons can be interpreted most reasonably in terms of a constant activation energy of approximately 260 kcal/mole and a range of k_0 values.

In any case, the effective activation-energy values for Stages I and II in pyrolytic carbons are very nearly the same. It has been shown above that Stage I consists primarily of layer ordering and that this process is rate-determining. During Stage II, layer ordering, crystallite diameter, and degree of preferred orientation are increasing simultaneously, but it seems likely that increase of one of the latter two parameters is rate-determining. Therefore, it appears that the effective activation energy for layer ordering and for reorientation and growth of crystallites are approximately the same. This conclusion is supported by reanalysis (by the superposition method) of published data on the kinetics of graphitization of

conventional carbons (Refs. 18, 48). In particular, data on magnetic susceptibility (in the range where L_a is increasing rapidly and c changes very little) (Ref. 3), crystallite height L_c (Ref. 9), and unit-cell height (Refs. 2, 15) all yield effective ΔH values in the neighborhood of 260 kcal/mole, within experimental error, for treatment temperatures above about 1800°C. Recently, Noda, Inagaki, and Hirano (Ref. 9) have reported that direct measurements of L_a and c kinetics in petroleum coke support the hypothesis that the activation energy is the same for both. Analysis of the high-temperature creep behavior of pyrolytic carbons also gives effective activation energies near 260 kcal/mole (Ref. 49). Thus there is considerable experimental evidence for a fundamental, thermally activated mechanism of mass transport in carbons and graphite with $\Delta H \simeq 260$ kcal/mole, which is rate-determining in a variety of high-temperature processes.

The large value of the activation energy observed here is consistent with the well known, very strong temperature dependence and the high temperature of occurrence of graphitization. However, the fundamental process with which it is associated is difficult to determine. Relatively little is known about the mechanisms of self-diffusion and diffusive mass transport in carbons and graphite. Kanter (Ref. 50) obtained experimentally a value of only 163 kcal/mole for self-diffusion parallel to the layer planes. It is possible that the graphitization activation energy corresponds to diffusion normal to the layer planes. Little theoretical or experimental attention appears to have been given to this problem, but the energy for diffusion normal to the layer planes would be expected to be higher than that for layer plane diffusion. Alternatively, more than one mechanism of layer plane diffusion may operate in graphite. According to Dienes (Ref. 51) direct interchange should be the lowest energy mechanism for self-diffusion. However, processes such as graphitization and creep must involve mass transport and thus require a mechanism such as vacancy or interstitialcy diffusion. On the basis of present information, 260 kcal/mole appears to be a reasonable activation energy for vacancy diffusion parallel to the layer planes. Dienes (Ref. 51), as corrected by Kanter (Ref. 50), calculated a vacancy diffusion energy of 263 kcal/mole. The excellent agreement with the observed energy for graphitization is probably fortuitous due to the difficulty of the rigorous theory and the many assumptions necessary. However, recent calculations of the vacancy formation energy by Coulson et al. (Refs. 52, 53) also support a high vacancy diffusion energy. Experimentally, Hennig (Refs. 54, 55) has deduced that the energy for vacancy formation is greater than 150 kcal/mole, while the vacancy migration energy is estimated by Baker and Kelley (Ref. 56) to be ~75 kcal/mole. These values are also consistent with a vacancy layer-plane diffusion activation energy greater than 200 kcal/mole.

Many of the features of the kinetics of graphitization of carbons can be rationalized qualitatively in terms of a simple model of the graphitization process. This model is based largely on concepts which were advanced earlier by Franklin (Ref. 57), Mrozowski (Refs. 40, 58), Mering and Maire (Ref. 37), Akamatu and Kuroda (Ref. 45), Mizushima (Ref. 44), and others. Assume that graphitization occurs by the translation and rotation of entire layer planes within a parallel stack. To accomplish this, the covalent carbon–carbon bonds linking the ordering plane with layer planes in adjacent crystallites must be rearranged. The energy increase associated with disordered layer stacking in graphite is quite small. This is shown by the large separations observed between dissociated partial dislocations in the basal plane, corresponding to a stacking fault energy of only 0.1 erg/cm² or less (Refs. 59, 60). The energy of the more random disorder found in turbostratic carbons may be somewhat higher, but may still be expected to be very modest. On the other hand, rearrangement of the peripheral bonds involves rather high energies, and probably requires extensive atomic rearrangement because of the directional character of carbon bonding. Therefore, the driving energy for layer ordering may be expected to be an increasing function of crystallite diameter. This is consistent with the observed dependence of degree of layer ordering on L_a illustrated schematically in Fig. 16. The rearrangement of the peripheral atoms may be expected to be the rate-determining process, consistent with the approximate equality of the activation energies for layer ordering and crystallite growth. With increasing L_a, the number of peripheral bonds which must be rearranged increases and the rate of layer ordering should decrease, as observed. Thus in small crystallites, layers can order rapidly, but the "equilibrium" degree of order is low; for large crystallites the "equilibrium" degree of order is high but the rate is low. The occurrence of a single, well defined rate process, as in Stage I of carbons A–E, implies a narrow distribution of crystallite sizes, in terms of this model. A distribution of rate constants could result from a distribution of crystallite sizes, or from a distribution of peripheral bonding conditions caused by the presence of voids or impurities at the crystallite boundaries. This model appears to imply a cooperative rearrangement of the peripheral atoms in the process of layer ordering. However, the actual process of graphitization is probably

much more complex than that represented here. Other detailed mechanisms not considered here, perhaps involving partial basal-plane dislocations, are probably involved. Nevertheless, the simple model outlined here provides a useful synthesis of many of the observed features of graphitization.

V. SUMMARY

The graphitization of pyrolytic carbons in the temperature range 2400–3000°C has been shown to be a thermally activated process with a single effective activation energy of approximately 260 kcal/mole. Available information suggests that the fundamental, thermally activated process may be diffusion parallel to the layer planes by a vacancy mechanism, but other possibilities such as diffusion normal to the layer planes cannot be ruled out. No evidence was found for true "saturation" at partial degrees of graphitization under isothermal heat treatment, or for a well-defined graphitization temperature. Furthermore, the fundamental graphitization process appeared to be the same in all of the pyrolytic carbons investigated. However, the detailed kinetic behavior depends on the initial microstructure of the carbon. Pyrolytic carbons with as-deposited apparent crystallite diameters larger than about 200 Å graphitize in a succession of first-order stages. This class of carbons includes most of those deposited under the usual conditions of temperature, pressure, flow rate, etc. The first stage involves primarily layer ordering, without crystallite growth or other marked microstructural changes, and is completed at a unit-cell height of approximately 6.74 Å. In the second stage, some additional layer ordering occurs (to about 6.72 Å) as a consequence of crystallite growth and there is a marked increase in preferred orientation. There is evidence for a third stage, in which the unit-cell height decreases to the graphite value of 6.708 Å, perhaps as a result of the removal of residual structural defects such as cone boundaries. Changes in optical microstructure and macroscopic dimensions occur primarily during Stages II and III and are largely a consequence of the other structural changes outlined above. The rate of layer ordering in Stage I decreases with increasing as-deposited crystallite diameter. The distinction between Stages I and II can be attributed to an apparent dependence of the "equilibrium" degree of layer order on L_a and the relatively large as-deposited L_a values found in many pyrolytic carbons. In pyrolytic carbons with as-deposited L_a values smaller than about 200 Å, and in regeneratively nucleated materials these individual stages are broadened and may not be resolved. The regenerative structure was found to be more stable than the substrate nucleated structure. This is probably due to the high structural disorder associated with soot particles incorporated in the deposit. A simple model of the graphitization process incorporating these features has been discussed.

In conclusion, some remarks may be made on the significance of the kinetic aspects of the high-temperature transformation in pyrolytic carbons for engineering applications of these materials. Appreciable changes in properties and dimensions are associated with the transformation, and it is necessary to assess the amount of transformation which may be expected under the conditions of interest. Some guidelines for this assessment may be sketched under the important restrictions of nonreactive ambient atmosphere and zero applied stress. The layer-ordering increase in Stage I may be expected to increase the electrical and, to a lesser extent, the thermal conductivity parallel to the substrate, but it should have little influence on the mechanical properties. Dimensional changes parallel to the substrate during Stage I are also small, but thickness decreases of 2–4% may be expected. A significant portion of Stage I may occur in a few hours at 2500°C and in a few seconds at 3000°C. During the later stages of the transformation, the large changes in preferred orientation and crystallite size will cause large changes in all of the properties of the carbon. In addition to changes in intrinsic properties, macroscopic property anisotropy will, of course, become much more pronounced. Significant Stage II effects are not likely to be realized in times shorter than one day at temperatures below 2700°C, but may occur in a few minutes at 3000°C. The pronounced microstructural changes and the completion of dimensional changes associated with Stage III require times of at least a few hours at 3000°C, but will occur in a few minutes at 3400°C. These conclusions

apply to substrate nucleated carbons under zero applied stress in nonreactive atmospheres. Regeneratively nucleated carbons tend to be much more stable. There is evidence that oxidizing atmospheres appreciably accelerate the graphitization process in conventional carbons (Ref. 8). This may also be true of pyrolytic carbons, though the denser structure and pronounced orientation texture of these carbons should moderate such effects. Finally, in the presence of externally applied stresses, the structural transformation may be considerably accelerated. High-temperature tensile deformation parallel to the substrate (Refs. 61–63), or compressive deformation normal to the substrate (Refs. 64, 65) greatly enhances the preferred-orientation increase and the microstructural changes with respect to that which is realized under the influence of thermal treatment alone. Heat treatment under high hydrostatic pressures greatly accelerates the graphitization process in a variety of carbon types, including those normally considered nongraphitizing (Refs. 66, 67).

While many of the significant kinetic aspects of the graphitization transformation have been identified in this investigation, much remains to be learned before the graphitization process is understood in detail. Further studies of the influence of microstructure, especially the parameter L_a, are needed; and the nature of the rate-determining, thermally activated process is still uncertain. Possible influences of heat-treatment technique on the results should be investigated further. The effect of stress or plastic deformation on the kinetics of graphitization is another area of interest. Further studies along these lines are planned.

APPENDIX A

Heat Treatment Time Correction

The ideal isothermal heat treatment is a square pulse of temperature vs time. The temperature should rise instantaneously, remain constant at the desired value for the desired time, then drop instantaneously to room temperature. In practice this cannot be achieved. The time–temperature record for an actual heat treatment is shown in Fig. A-1a. The broken-line rectangle outlines the nominal (ideal) treatment (2600°C for 10 min). It is necessary to make corrections for the finite heat-up and cool-down times and any other deviations of the actual temperature from the desired value.

If the property P being studied is thermally activated and the effective activation energy ΔH is known approximately, the correction may be made as follows. It can be shown by a simple argument that the value of P after a series of incremental heat treatments at absolute temperature T_i for time intervals Δt_i is given by

$$P = P_0 \exp\left[-\sum_i k(T_i)\,\Delta t_i\right] \qquad \text{(A-1)}$$

where P_0 is the initial value of P,

$$k(T_i) = k_0 \exp\left(-\Delta H/RT_i\right)$$

is the rate constant, R is the gas constant and k_0 is a constant. Now a treatment at T_i for time Δt_i is equivalent to a treatment at the desired temperature T_0 for an interval $\Delta t'_i$

$$k(T_i)\,\Delta t_i = k(T_0)\,\Delta t'_i \qquad \text{(A-2)}$$

and Eq. (A-1) can be rewritten in the form

$$P = P_0 \exp\left[-k(T_0)\,t_0\right]$$

where $t_0 = \sum_i \Delta t'_i$. Rearranging (A-2) and substituting the definition of $k(T)$, in (A-2), $\Delta t'_i$ is given by

$$\Delta t'_i = \Delta t_i \exp\left[\Delta H/R\,(1/T_0 - 1/T_i)\right] = \Delta t_i \exp(x_i)$$

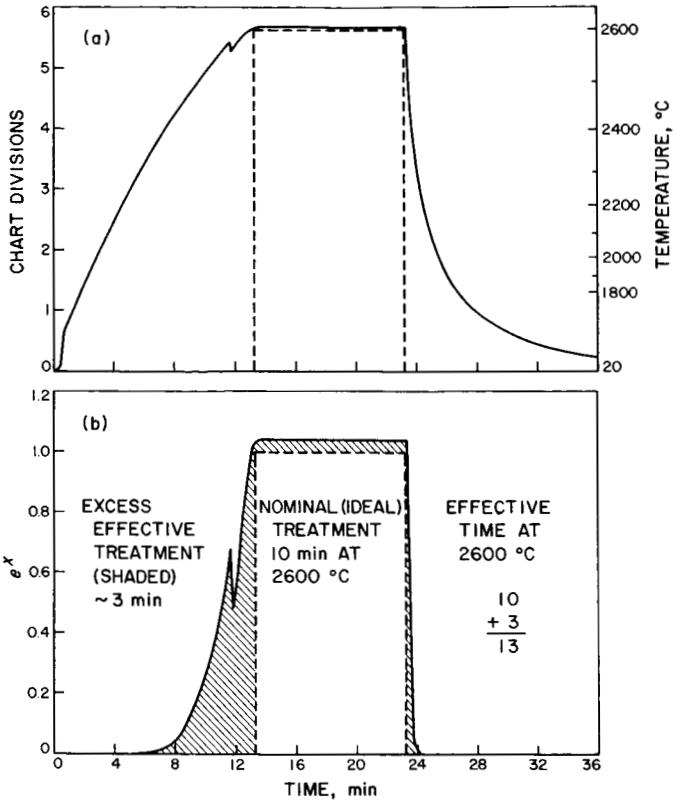

Fig. A-1. Heat-treatment time correction: (a) actual (solid line) and ideal (broken line) treatment profiles; (b) effective treatment profile

where

$$x_i = \Delta H/R\,(1/T_0 - 1/T_i)$$

Here t_0 is the effective or equivalent treatment time at T_0, and the summation is carried out over the entire treatment period, including heat-up and cool-down. Although the procedure has been described in terms of a single first-order rate process, it should also apply to the case of a distribution of first-order processes if ΔH and the distribution of pre-exponential factors are temperature-independent.

The corrected or effective heat-treatment time t_0 may be determined graphically by plotting $\exp(x)$ against treatment time, as shown in Fig. A-1b, and measuring the area under the curve. A value of $\Delta H = 260$ kcal/mole was used. In general, a sufficiently accurate value of ΔH for this correction can be determined from the uncorrected measurements made at long treatment times. If the temperature does not deviate appreciably from the desired value during the isothermal period, the correction results largely from the heat-up time and amounts to only a few minutes. In addition, the correction is not especially sensitive to the value of ΔH used. In the example shown, changing ΔH over the range of 200–300 kcal/mole changed the correction by only ± 0.2 min. Application of this correction procedure to the present data served principally to reduce the scatter; no significant change in the results or the interpretation resulted.

APPENDIX B

Sample Size Effects

The x-ray unit-cell height and crystallite diameter measurements were made on heat-treated powders (about 40 μ) while preferred-orientation data were obtained on $1 \times 1 \times 10$-mm^3 sticks and the magnetic-susceptibility measurements were made on cubes about 3 mm on a side. An investigation was therefore made to determine whether or not the graphitization behavior was influenced by sample size. Some c-spacing and L_a measurements were made on the solid-stick preferred-orientation samples, using a Debye–Scherrer camera. The same general behavior was observed for these samples as for the powder, but both c and L_a tended to be smaller in the solid samples during the later stages of graphitization. Stage I results were not reliable for the stick samples as discussed in Section II. To determine if this was a real effect, powder samples were taken from a number

of annealed magnetic-susceptibility specimens. In all cases, the c values from these samples agreed well with the annealed-powder results, but again L_a values were lower.

A careful examination of these data suggests that the low values obtained from the stick samples are largely a result of absorption effects which shift the diffracted intensity peaks to slightly higher angles (Ref. 68). The absorption factor $A = I/I_0$ for the solid sticks is about half that for the capillary powder samples, and the discrepancy in c values is largely removed by plotting c against $\frac{1}{2}(\cos^2\theta/\sin\theta + \cos^2\theta/\theta)$ and extrapolating to zero on the abscissa (Refs. 69, 70). On the other hand, filing to produce powder from the susceptibility samples evidently reduces L_a toward the as-deposited value without noticeably increasing c. The reduction of L_a by filing is consistent with results of fine-grinding experiments, but extensive grinding also increases c (Refs. 71, 72). It has been found here that filing does not appear to affect c, though in well-graphitized samples (c less than about 6.72 Å) it produces fairly strong rhombohedral lines. These can be removed by annealing the powder (15 min at 2900–3000°C) but no detectable change in c is produced by this treatment. These effects of absorption and sample preparation are apparently sufficiently large to mask any true differences in graphitization behavior due to sample size in the range considered. If a sample-size effect does exist, it is evidently small.

APPENDIX C

Macroscopic Dimensional Changes

Pyrolytic carbons undergo irreversible changes in macroscopic dimensions as a result of heat treatment. These changes consist of growth parallel to the substrate surface and shrinkage perpendicular to it. Stover (Ref. 73) pointed out that these dimensional changes are closely related to the microstructure and the degree of preferred orientation of the carbon. Changes in all of these properties are manifestations of the "dewrinkling" of the structure. Therefore, dimensional changes may be expected to occur primarily during the second and later stages of graphitization. No data on dimensional changes were obtained in this investigation, but results of Richardson and Zehms (Ref. 15), Kotlensky and Martens (Ref. 74), and Carlsen (Ref. 75) are in general accord with these expectations, as shown in Fig. C-1. Using a simple wrinkled sheet model, it can be shown that the maximum expansion parallel to the deposition plane is $\Delta l/l \sim 1/2n \sim [(\cos\langle\omega^2\rangle_{ar}^{\frac{1}{2}})^{-1} - 1]$ where n is the preferred-orientation parameter. Since n is approximately 10 for most as-deposited pyrolytic carbons, the maximum $\Delta l/l$ for these materials is about 5%. Reported values range from 4 to 5%. The expected dimensional change normal to the substrate is more difficult to predict. An approximately 2% decrease in thickness results from the decrease in unit-cell height. The additional shrinkage resulting from dewrinkling cannot be calculated without a more detailed specification of the microstructure. The "wavelength" of the wrinkles, which is closely related to the average growth cone size, is the important parameter. Thickness decreases as large as 16% have been observed.

It has also been observed that annealing-induced dimensional changes occur much less rapidly in regenerative-type structures than in substrate nucleated structures, in agreement with the present observations on preferred orientation and microstructure changes.

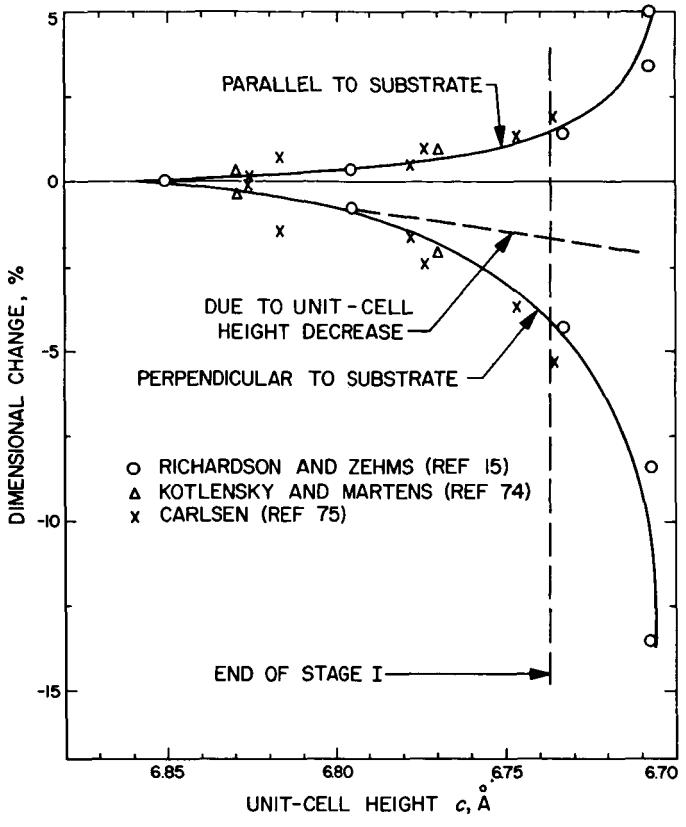

Fig. C-1. Macroscopic dimensional change as a function of unit-cell height

NOMENCLATURE

a	Unit-cell width
a'	Apparent a determined from position of maximum intensity of an (hk) diffraction band
c	Unit-cell height
c_0	Initial unit-cell height
c_1	Unit-cell height at end of Stage I
c_2	Unit-cell height at end of Stage II
g	Degree of graphitization, expressed as fractional change in unit-cell height
I	Diffraction peak intensity
k	Rate constant
k_0	Pre-exponential factor of rate constant
k_1	Stage I rate constant
k_2	Stage II rate constant from susceptibility and unit-cell height data
k_2'	Rate constant from preferred-orientation data
$K(T)$	Boltzmann factor $\exp(-\Delta H/RT)$
L_a	Apparent crystallite layer diameter

NOMENCLATURE (Cont'd)

n	Preferred-orientation parameter
n_0	Initial (as-deposited) preferred-orientation parameter
n_∞	Final preferred-orientation parameter
R	Gas constant
t	Total treatment time
T	Absolute temperature
T_0	Arbitrary reference temperature
ΔH	Effective activation energy
θ	Bragg angle of diffraction maximum
λ	X-ray wavelength
χ_a	Diamagnetic susceptibility parallel to layer planes of crystallite
χ_c	Diamagnetic susceptibility perpendicular to layer planes of crystallite
$\chi_{\parallel}$	Diamagnetic susceptibility parallel to substrate plane
$\chi_{\perp}$	Diamagnetic susceptibility perpendicular to substrate plane
χ_T	Total (trace) diamagnetic susceptibility
χ_0	Initial (as-deposited) total diamagnetic susceptibility
χ_{min}	Minimum (end of Stage I) total diamagnetic susceptibility
χ_∞	Final (graphite) total diamagnetic susceptibility

REFERENCES

1. Freise, E. J., and Kelley, A., "The Deformation of Graphite Crystals and the Production of the Rhombohedral Form," *Philosophical Magazine*, Vol. 8, 1963, pp. 1519–1523.
2. Fair, F. V., and Collins, F. M., "Effect of Residence Time on Graphitization at Several Temperatures," *Proceedings of the Fifth Conference on Carbon*, Vol. 1, New York: Pergamon Press, 1962, pp. 503–508.
3. Mazza, M., Marchand, A., and Pacault, A., "Contribution à l'étude cinetique de la graphitation," *Journal de chimie physique et de physicochimie biologique*, Vol. 59, 1962, pp. 657–658.
4. Mizushima, S., "Rate of Graphitization of Carbon," *Proceedings of the Fifth Conference on Carbon*, Vol. 2, New York: Pergamon Press, 1962, pp. 439–447.
5. Mazza, M., "Contribution à l'étude cinetique de la graphitation. I. Étude magnétique," *Journal de chimie physique et de physicochimie biologique*, Vol. 61, 1964, pp. 721–728.
6. Mazza, M., Gasparoux, H., and Amiell, J., "Contribution à l'étude cinetique de la graphitation. II. Deuxième mémoire," Ibid., pp. 729–732.

REFERENCES (Cont'd)

7. Forchioni, A., Boisard, F., and Delhaes, P., "Contribution à l'étude cinetique de la graphitation. III. Troisième mémoire," Ibid., pp. 1289–1295.

8. Noda, T., Inagaki, M., and Sekiya, T., "Effect of Ambient Gas Phase on Graphitization Rate of Carbon," Symposium on Carbon, Tokyo, Japan, July 1964, Paper III-24.

9. Noda, T., Inagaki, M., and Hirano, S., "Kinetic Studies on Graphitization: Effect of Thermal History of Carbon on Rate of Graphitization," Seventh Carbon Conference, Cleveland, June 1965, Paper 128.

10. Tarpinian, A., and Tedman, C., *An Analysis of Carbon Crystallite Growth Kinetics during Graphitization,* Watertown, Massachusetts: Watertown Arsenal Laboratories, November 1962, WAL TR 851.5/1.

11. Pacault, A., private communication.

12. Noda, T., private communication.

13. Guentert, O. J., and Cvikevich, S., "X-ray Study of the Effects of Heat Treatment on Pyrolytic Graphites," *Proceedings of the Fifth Congress on Carbon,* Vol. 1, New York: Pergamon Press, 1962, pp. 473–484.

14. Bragg, R. H., and Packer, C. M., "Orientation Dependence of Structure in Pyrolytic Graphite," *Nature,* Vol. 195, 1962, pp. 1080–1082.

15. Richardson, J. H., and Zehms, E. H., *Structural Changes in Pyrolytic Graphite at Elevated Temperatures,* El Segundo, California: Aerospace Corporation, September 1963, Report SSD-TDR 63-340 (TDR-269 (4240-10)-3).

16. Fischbach, D. B., "Kinetics of High-Temperature Structural Transformation in Pyrolytic Carbons," *Applied Physics Letters,* Vol. 3, 1963, pp. 168–170.

17. Fischbach, D. B., "The Kinetics of the Transformation of Pyrolytic Carbons," *Proceedings of the ASTM Symposium on Pyrolytic Graphite, Palm Springs, March 1964,* to be published.

18. Fischbach, D. B., "Observations on the Kinetics of Graphitization: I. Dependence of Graphitization on Heat Treatment Time; II. The Activation Energy and mechanism of Graphitization," Symposium on Carbon, Tokyo, Japan, July 1964, Papers III-22, III-23.

19. Horton, W. S., "Oxidation Kinetics of Pyrolytic Graphite," Proceedings of the *Fifth Conference on Carbon,* Vol. 2, New York: Pergamon Press, 1963, pp. 233–241.

20. Smith, W. H., private communication.

21. Warren, B. E., "X-ray Diffraction in Random Layer Lattices," *Physical Review,* Vol. 59, 1941, pp. 693–698.

22. Bacon, G. E., and Franklin, R. E., "The a Dimension of Graphite," *Acta Crystallographica,* Vol. 4, 1951, p. 561.

23. Guentert, O. J., and Klein, C. A., "Preferred Orientation and Anisotropy Ratio of Pyrolytic Graphite," *Applied Physics Letters,* Vol. 2, 1963, pp. 125–127.

REFERENCES (Cont'd)

24. Guentert, O. J., "X-ray Study of Pyrolytic Graphite," *Journal of Chemical Physics,* Vol. 37, 1962, pp. 884–891.

25. Fischbach, D. B., "Kinetics of Graphitization," *Jet Propulsion Laboratory Space Programs Summary No. 37-24,* Vol. IV, December 1963, pp. 44–45.

26. Fischbach, D. B., "The Kinetics of Graphitization," Jet Propulsion Laboratory *Space Programs Summary No. 37-31,* Vol. IV, February 1965, pp. 103–105.

27. Fischbach, D. B., "On the Structure-Sensitivity of the Diamagnetism of Pyrolytic Carbons," Seventh Conference on Carbon, Cleveland, June 1965, Paper 77.

28. Fischbach, D. B., "Diamagnetic Susceptibility of Pyrolytic Graphite," *Physical Review,* Vol. 123, 1961, pp. 1613–1614.

29. Fischbach, D. B., "The Magnetic Susceptibility of Pyrolytic Carbons," *Proceedings of the Fifth Conference on Carbon,* Vol. 2, New York: Pergamon Press, 1963, pp. 27–36.

30. Poquet, E., "Structure et propriétés diamagnétique des pyrocarbones," *Journal de chimie physique et de physicochimie biologique,* Vol. 60, 1963, p. 566.

31. Fischbach, D. B., "The Magnetic Properties of Pyrolytic Carbons," *Proceedings of the ASTM Symposium on Pyrolytic Graphite, Palm Springs, March 1964,* to be published.

32. Diefendorf, R. J., private communication.

33. Fischbach, D. B., unpublished.

34. Sutter, P. H., and Nowick, A. S., "Ionic Conductivity and Time-Dependent Polarization in NaCl Crystals," *Journal of Applied Physics,* Vol. 34, 1963, pp. 734–746.

35. Kotlensky, W. V., and Walker, P. L., Jr., "Crystallographic and Physical Changes of Some Carbons upon Oxidation and Heat Treatment," *Proceedings of the Fourth Conference on Carbon,* New York: Pergamon Press, 1960, pp. 423–442.

36. Schaeffer, W. D., Smith, W. R., and Polley, M. H., "Structure and Properties of Carbon Blacks — Changes Induced by Heat Treatment," *Industrial and Engineering Chemistry,* Vol. 45, 1953, pp. 1721–1725.

37. Mering, J., and Maire, J., "Le processus de la graphitation," *Journal de chimie physique et de physicochimie biologique,* Vol. 57, 1960, pp. 803–812.

38. Maire, J., and Mering, J., "Croissance des dimensions des domaines crystallins au cours de la graphitation de carbone," *Proceedings of the Fourth Conference on Carbon,* New York: Pergamon Press, 1960, pp. 345–350.

39. Takahashi, H., Kuroda, H., and Akamatu, H., "Correlation between Stacking Order and Crystallite Dimensions in Carbons," *Carbon,* Vol. 2, 1965, pp. 432–433.

40. Mrozowski, S., "Mechanical Strength, Thermal Expansion and Structure of Cokes and Carbons," *Proceedings of the First and Second Conferences on Carbon,* Baltimore: The Waverly Press, 1956, pp. 31–45.

REFERENCES (Cont'd)

41. Yang, K. T., "The Determination of the Interlayer Spacings in Carbons at High Temperature," *Proceedings of the Fifth Conference on Carbon,* Vol. 1, New York: Pergamon Press, 1962, pp. 492–496.

42. Entwisle, F., "Thermal Expansion of Pyrolytic Graphite," *Physics Letters,* Vol. 2, 1962, pp. 236–238.

43. Tsuzuku, T., "Graphitization Stresses and Dislocations in Polycrystalline Carbon," *Proceedings of the Fourth Conference on Carbon,* New York: Pergamon Press, 1960, pp. 403–416.

44. Mizushima, S., "On the Crystallite Growth of Carbon," Ibid., pp. 417–421.

45. Akamatu, H., and Kuroda, H., "On the Substructure and the Crystallite Growth in Carbon," Ibid., pp. 355–369.

46. Nowick, A. S., "A Reinterpretation of Experiments on Intermetallic Diffusion," *Journal of Applied Physics,* Vol. 22, 1951, pp. 1182–1186.

47. Fischbach, D. B., "Kinetics of Graphitization of a Petroleum Coke," *Nature,* Vol. 200, 1963, pp. 1281–1283.

48. Fischbach, D. B., "The Kinetics of Graphitization," *Jet Propulsion Laboratory Space Programs Summary No. 37-25,* Vol. IV, February 1964, pp. 43–45.

49. Kotlensky, W. V., "Analysis of High Temperature Tensile Creep Parallel to Substrate in Pyrolytic Graphite," Seventh Conference on Carbon, Cleveland, June 1965, Paper 66; also, *Jet Propulsion Laboratory Space Programs Summary No. 37-30,* Vol. IV, December 1964, pp. 71–72.

50. Kanter, M. A., "Diffusion of Carbon Atoms in Natural Graphite Crystals," *Physical Review,* Vol. 107, 1957, pp. 655–663; "The Mechanism of Atom Motion in Graphite Crystals," *Kinetics of High Temperature Processes,* Kingery, W. D. (editor), New York: John Wiley & Sons, 1959, pp. 61–66.

51. Dienes, G. J., "Mechanism for Self-Diffusion in Graphite," *Journal of Applied Physics,* Vol. 23, 1952, pp. 1194–1200.

52. Coulson, C. A., Herraez, M. A., Leal, M., Santos, E., and Sennent, S., "Formation Energy of Vacancies in Graphite Crystals," *Proceedings of the Royal Society* (London), Vol. A274, 1963, pp. 461–479.

53. Coulson, C. A., and Poole, M. D., "Calculation of Formation Energy of Vacancies in Graphite Crystals," *Carbon,* Vol. 2, 1964, pp. 275–279.

54. Hennig, G. R., "Vacancies and Dislocation Loops in Graphite," *Applied Physics Letters,* Vol. 1, 1962, pp. 55–56.

55. Hennig, G., "Vacancies and Dislocation Loops in Quenched Crystals of Graphite," *Journal of Applied Physics,* Vol. 36, 1965, pp. 1482–1486.

56. Baker, C., and Kelly, A., "Energy to Form and to Move Vacant Lattice Sites in Graphite," *Nature,* Vol. 193, 1962, pp. 235–236.

57. Franklin, R. E., "Crystallite Growth in Graphitizing and Nongraphitizing Carbons," *Proceedings of the Royal Society (London),* Vol. A209, 1951, pp. 196–218.

REFERENCES (Cont'd)

58. Mrozowski, S., "Kinetics of Graphitization," *Kinetics of High Temperature Processes*, Kingery, W. D. (editor), New York, John Wiley & Sons, 1959, pp. 264–270.

59. Williamson, G. K., "Electron Microscope Studies of Dislocation Structures in Graphite," *Proceedings of the Royal Society (London)*, Vol. A257, 1960, pp. 457–463.

60. Amelinckx, S., and Delavignette, P., "Electron Optical Study of Basal Dislocations in Graphite," *Journal of Applied Physics*, Vol. 31, 1960, pp. 2126–2135.

61. Bragg, R. H., Crooks, D. D., Fenn, R. W., Jr., and Hammond, M. L., "The Effect of Applied Stress on the Graphitization of Pyrolytic Graphite," *Carbon*, Vol. 1, 1964, pp. 171–179.

62. Kotlensky, W. V., and Martens, H. E., "Structural Changes Accompanying Deformation in Pyrolytic Graphite," *Journal of the American Ceramics Society*, Vol. 48, 1965, pp. 135–138.

63. Kotlensky, W. V., and Martens, H. E., *Structural Transformation in Pyrolytic Graphite Accompanying Deformation*, Pasadena, California: Jet Propulsion Laboratory, November 1962, Technical Report No. 32-360.

64. Ubbelohde, A. R., Young, D. A., and Moore, A. W., "Annealing of Pyrolytic Graphite under Pressure," *Nature*, Vol. 198, 1963, pp. 1192–1193.

65. Gremion, R., and Maire, J., "Modification de la structure du carbone pyrolytique par compression à haute temperature-evolution vers le monocristal," Sixth Conference on Carbon, Pittsburgh, June 1963, Paper 14.

66. Noda, T., and Kato, H., "Heat Treatment of Carbon under High Pressure," Symposium on Carbon, Tokyo, Japan, July 1964, Paper III-19.

67. Noda, T., Inagaki, M., Kato, H., Amanuma, A., and Kamiya, K., "Heat Treatment of Carbon under Pressure," Seventh Conference on Carbon, Cleveland, June 1965, paper 129.

68. Taylor, A., and Sinclair, H., "The Influences of Absorption on the Shapes and Positions of Lines in Debye–Scherrer Powder Photographs," *Proceedings of the Physical Society (London)*, Vol. 57, 1945, pp. 108–125.

69. Nelson, J. B., and Riley, D. P., "An Experimental Investigation of Extrapolation Methods in Derivation of Accurate Unit-Cell Dimensions of Crystals," Ibid., pp. 160–177.

70. Taylor, A., and Sinclair, H., "On the Determination of Lattice Parameters by the Debye–Scherrer Method," Ibid., pp. 126–135.

71. Bacon, G. E., "X-ray Diffraction Studies of Irradiated and Ground Graphites," *Proceedings of the Third Conference on Carbon*, New York: Pergamon Press, 1959, pp. 475–480.

72. Walker, P. L., Jr., and Seeley, S. B., "Fine Grinding of Ceylon Natural Graphite," *Proceeding of the Third Conference on Carbon*, New York: Pergamon Press, 1959, pp. 481–494.

REFERENCES (Cont'd)

73. Stover, E. R., *Effects of Annealing on the Structure of Pyrolytic Graphite*, Schenectady, New York: General Electric Company, Research Laboratory, November 1960, Report No. 60-RL-2564M.

74. Kotlensky, W. V., and Martens, H. E., *Tensile Properties of Pyrolytic Graphite to 5000°F*, Pasadena, California: Jet Propulsion Laboratory, March 1961, Technical Report No. 32-71.

75. Carlson, F., Jr., *Effect of Pyrolytic Graphite Structure on Diffusion of Thorium*, Oak Ridge, Tennessee: Oak Ridge National Laboratory, June 1965, ORNL-TM-1080.

ACKNOWLEDGMENTS

It is a pleasure to thank H. E. Martens and W. V. Kotlensky for helpful discussions during the course of these studies; and O. Kilham and T. Baugh (magnetic susceptibility), S. Kotake and T. Rogacs (x-ray diffraction), J. Adkins (microstructures), and L. Gnewuch (heat treatments) for assistance in taking the data. Special thanks are due to O. J. Guentert, Raytheon Company, for supplying samples of pyrolytic carbon of known crystallite size; and to R. J. Diefendorf, General Electric Company, and D. Schiff, High Temperature Materials, Inc., for supplying some of the pyrolytic carbons studied.